OAK RIDGE NATIONAL LABORATORY LIBRARIES
3 4456 0571563 3

ORNL/Sub-2913/7
Dist. Category NRC-5

END EFFECTS ON ELBOWS SUBJECTED TO MOMENT LOADINGS

E. C. Rodabaugh
S. K. Iskander
S. E. Moore

Work funded by
U.S. Nuclear Regulatory Commission
Office of Nuclear Regulatory Research
Under Interagency Agreements 40-551-75 and 40-552-75

If you wish someone else to see this report, send in name with report and the library will arrange a loan.
UCN 7969 (3 9-77)

March, 1978

Work Performed by

BATTELLE
Columbus Laboratories
505 King Avenue
Columbus, Ohio 43201

for
OAK RIDGE NATIONAL LABORATORY
Oak Ridge, Tennessee 37830
operated by
UNION CARBIDE CORPORATION
for the
ENERGY RESEARCH AND DEVELOPMENT ADMINISTRATION

Contract No. W-7405-eng-26

C-78d

Printed in the United States of America
Available from
National Technical Information Service
U.S. Department of Commerce
5285 Port Royal Road
Springfield, Virginia 22151
Price: Printed Copy $4.50; Microfiche $3.00

This report was prepared as an account of work sponsored by the United States Government. Neither the United States nor the Energy Research and Development Administration, nor the Nuclear Regulatory Commission, nor any of their employees, nor any of their contractors, subcontractors, or their employees, makes any warranty, express or implied, or assumes any legal liability or responsibility for the accuracy, completeness or usefulness of any information, apparatus, product or process disclosed, or represents that its use would not infringe privately owned rights.

ORNL/Sub-2913/7
Dist. Category NRC-5

END EFFECTS ON ELBOWS SUBJECTED TO MOMENT LOADINGS

by

E. C. Rodabaugh
S. K. Iskander
S. E. Moore

Manuscript Completed: March, 1978

Date Published: March 1978

NOTICE This document contains information of a preliminary nature and was prepared primarily for internal use at the Oak Ridge National Laboratory. It is subject to revision or correction and therefore does not represent a final report

Work funded by
U.S. Nuclear Regulatory Commission
Office of Nuclear Regulatory Research
Under Interagency Agreements 40-551-75 and 40-552-75

TABLE OF CONTENTS

	Page
FOREWORD	ii
ABSTRACT	v
NOMENCLATURE	vi
1. INTRODUCTION	1
2. SCOPE	6
3. FINITE ELEMENT MODEL	7
4. VALIDATION OF FINITE ELEMENT MODEL	8
5. STRESSES	10
In-Plane Moment	10
Out-of-Plane Moment	11
6. FLEXIBILITY FACTORS	13
In-Plane Moment	13
Out-Of-Plane Moment	14
7. DESIGN GUIDANCE	17
Maximum Stresses	17
Flexibility Factors	20
Recommended Code Rules	21
Discussion of Recommendations	24
8. STRESSES AT WELDS	27
9. SUMMARY	29
10. REFERENCES	30
Figures in Numerical Order	32-51
Tables in Numerical Order	52-63

FOREWORD

The work reported here was performed at Oak Ridge National Laboratory and at Battelle-Columbus Laboratories under Union Carbide Corporation, Nuclear Division, Subcontract No. 2913 in support of the ORNL Design Criteria for Piping and Nozzles Program being conducted for the U.S. Nuclear Regulatory Commission, Office of Nuclear Regulatory Research. E. K. Lynn of the Metallurgy and Materials Branch, Division of Reactor Safety Research, USNRC is the cognizant rsr engineer and S. E. Moore of the Oak Ridge National Laboratory, Division of Engineering Technology (formerly Reactor Division) is the program manager.

The objectives of the ORNL program are to conduct integrated expermental and analytical stress analysis studies of piping system components and pressure vessel nozzles in order to confirm and/or improve the adequacy of structural design criteria and analytical methods used to assure the safe design of nuclear power plants. Activities under the program are coordinated with other safety related piping and pressure-vessel research through the Design Division, Pressure Vessel Research Committee (PVRC) of the Welding Research Council and through the ASME Boiler and Pressure Vessel Code Committees. Results from the ORNL program are used by appropriate Codes' and Standards' groups in drafting new or improved design rules and criteria.

The following reports have been issued under U.S. Nuclear Regulatory Commission sponsorship:

J. W. Bryson, J. P. Callahan, and R. C. Gwaltney, "Stress Analyses of Flat Plates with Attached Nozzles, Vol. 1. Comparison of Stresses in a One-Nozzle-to-Flat-Plate Configuration and in a Two-Nozzle Configuration with Theoretical Predictions", ORNL-5044 (July 1975).

R. L. Battiste et al., "Stress Analysis of Flat Plates with Attached Nozzles, Vol. 2., "Esperimental Stress Analyses of a Flat Plate with One Nozzle Attached," ORNL-5044 (July, 1975).

R. C. Gwaltney, J. W. Bryson, and S. E. Bolt, "Theoretical and Experimental Stress Analyses of ORNL Thin-Shell Cylinder-to-Cylinder Model 2", ORNL-5021 (October 1975).

E. C. Rodabaugh and S. E. Moore, "Stress Indices for ANSI Standard B16.11 Socket-Welidng Fittings", ORNL/TM-4929 (August 1975).

S. E. Moore, "Contributions of the ORNL Piping Program to Nuclear Piping Design Codes and Standards", Proceedings of the The Technology Information Meeting on Methods for Analyzing Piping Integrity, Nov. 11-12, 1975, ERDA-76-50; also in J. Press. Vessel Technol., Trans. ASME 99, 224-30 (February 1977).

W. L. Greenstreet, "Summary and Accomplishments of the ORNL Program for Nuclear Piping Design Criteria", Proceedings of the Technology Information Meeting on Methods for Analyzing Piping Integrity, Nov. 11-12, 1975, ERDA 76-50.

J. W. Bryson and W. F. Swinson, "Stress Analyses of Flat Plates with Attached Nozzles, Vol. 3., Experimental Stress Analyses of a Flat Plate with Two Closely Spaced Nozzles of Equal Diameter Attached", ORNL-5044 (December 1975).

E. C. Rodabaugh, F. M. O'Hara, Jr., and S. E. Moore, "FLANGE: A Computer Program for the Analysis of Flanged Joints with Ring-Type Gaskets", ORNL-5035, (January 1976).

R. E. Textor, User's Guide for "SHFA: Steady-State Heat Flow Analysis of Tee Joints by the Finite Element Method", UCCND/CSD/INF-60, Oak Ridge Gaseous Diffusion Plant (January 1976).

E. C. Rodabaugh and S. E. Moore, "Flanged Joints with Contact Outside the Bolt Circile - ASME Part B Design Rules", ORNL/Sub/2913-1, Battelle-Columbus Laboratories (May, 1976).

E. C. Rodabaugh, "Appropriate Nominal Stresses for Use With ASME Code Pressure-Loading Stress Indices for Nozzles", ORNL/Sub/2913-2, Battelle-Columbus Laboratories (June 1976).

S. E. Moore and J. W. Bryson, "Progress Report for the Design Criteria for Piping and Nozzles Program for the Two Quarterly Periods July 1 to Sept. 30 and Oct. 1 to Dec. 31, 1975", ORNL/NUREG/TM-18 (June 1976).

R. L. Maxwell and R. W. Holland, "Experimental Stress Analysis of the Attachment Region of a Hemispherical Shell with a Radially Attached Nozzle, Zero Penetration", ORNL/Sub/2203-4, University of Tennessee (July 1976).

J. P. Callahan and J. W. Bryson, "Stress Analyses of Perforated Flat Plates Under In-Plane Loadings", ORNL/NUREG-2 (August 1976).

E. C. Rodabaugh and S. E. Moore, "Evaluation of the Bolting and Flanges of ANSI B16.5 Flanged Joints - ASME Part A Flanges", ORNL/Sub/2913-3, Battelle-Columbus Laboratories (September 1976).

E. C. Rodabaugh and R. C. Gwaltney, "Elastic Stresses at Reinforced Nozzles in Spherical Shells with Pressure and Moment Loading", ORNL/Sub/2913-4, Battelle-Columbus Laboratories (October, 1976).

E. C. Rodabaugh, S. E. Moore, and J. N. Robinson, "Dimensional Control of Buttwelding Pipe Fittings for Nuclear Power Plant Class 1 Piping Systems", ORNL/Sub/2913-5, Battelle-Columbus Laboratories (December 1976).

S. E. Moore and J. W. Bryson, "Design Criteria for Piping and Nozzles Program Quarterly Progress Report for April-June 1976", ORNL/NUREG/TM-107 (April 1977).

E. C. Rodabaugh and S. E. Moore, "Flexibility Factors for Small (d/D < 1/3) Branch Connections with External Loadings", ORNL/Sub/2913-6, Battelle-Columbus Laboratories (March 1977).

S. E. Moore and J. W. Bryson, "Design Criteria for Piping and Nozzles Program Quarterly Progress Report for July-September 1976", ORNL/NUREG/TM-91 (February 1977).

P. G. Fowler and J. W. Bryson, "User's Manual for the CORTES Graphics Package GRFPAK", ORNL/NUREG/TM-127 (August 1977).

B. R. Bass, J. W. Bryson, and S. E. Moore, "Validation of the Finite Element Stress Analysis Computer Program CORTES-SA for Analyzing Piping Tees and Pressure Vessel Nozzles", Pressure Vessels and Piping Computer Program Evaluation and Qualification, RVP-PB-024, pp. 9-25, ASME (1977).

J. K. Hayes and S. E. Moore, "Experimental Stress Analysis for Four 24-in. ANSI Standard B16.9 Tees", Paper 77-PVP-4, presented at the ASME Energy Technology Conference and Exhibition, Houston, Tex., Sept. 18-23, 1977.

J. W. Bryson, W. G. Johnson, and B. R. Bass, "Stresses in Reinforced Nozzle-Cylinder Attachments Under Internal Pressure Loading Analyzed by the Finite-Element Method - A Parameter Study", ORNL/NUREG-4 (October, 1977).

F. K. W. Tso et al., "Stress Analysis of Cylindrical Pressure Vessels with Closely Spaced Nozzles by the Finite-Element Method, Vol. 1. Stress Analysis of Vessels with Two Closely Spaced Nozzles Under Internal Pressure", ORNL/NUREG-18/V1 (November 1977).

W. L. Greenstreet, "Experimental Study of Plastic Responses of Pipe Elbows", ORNL/NUREG-24 (February 1978).

ABSTRACT

End effects on elbows subjected to moment loading are investigated using the finite element program EPACA. Parameters covered are R/r = 2 or 3, α_o = 45", 90°, or 180°, "long" straight pipe attached to the ends of the elbows.

Relatively simple but more accurate (than present Code) equations are developed and recommendation for an alternative Code method using these equations is presented.

Data from EPACA on stresses at welds (elbow-to-pipe juncture) are presented. A simple equation is given for estimating the maximum stresses at the welds.

NOMENCLATURE

C_2 = stress index for moment loading used in Code

D_o = nominal outside diameter

D_{max}, D_{min}, D = maximum, minimum and average diameter, respectively, of an out-of-round elbow cross section

E = modulus of elasticity

G = shear modulus of elasticity

$h = tR/r^2$

I = moment in inertia

J = polar moment of inertia

k = flexibility factor.

k_i, k_o, k_t = flexibility factor for in-plane, out-of-plane and torsional moments, respectively

L = length of straight pipe, see Figure 1.

M = moment

M_i, M_o, M_t = in-plane, out-of-plane, torsional moment, respectively

M_1, M_2, M_3 = Code definition of moments, $M_1 = M_o$, $M_2 = M_i$, $M_3 = M_t$

$\overline{M} = (M_1^2 + M_2^2 + M_3^2)^{1/2}$

p = wall thickness variation coefficient

R = elbow bend radius, see Figure 1

r = elbow mid-wall cross section radius

r_f = radius of flange, see Figure 1

NOMENCLATURE
(Continued)

$S_n = M/\pi r^2 t$, nominal stress

t = wall thickness

t_f = thickness of flange, see Figure 1

x, y, z = coordinates, see Figure 1

α = coordinate angle, see Figure 1

α_o = arc angle of elbow, see Figure 1

$\gamma = EI/GJ = 1.3$ for Poisson's ratio = 0.3 used herein

δ_x, δ_y, δ_z = displacements in directions x, y, and z

θ_x, θ_y, θ_z = rotations in directions x, y, and z

$\lambda = tR/[r^2(1-\nu^2)^{1/2}]$

ν = Poisson's ratio

σ = normal stress

σ_{max} = maximum stress

σ_{mi} = maximum stress by interpolation of EPACA calculations

$\bar{\sigma}$ = stress intensity

$\sigma_{mc} = 1.95/h^{2/3}$

σ_w = maximum stress at weld (elbow-to-pipe juncture)

τ = shear stress

ϕ = coordinate angle, see Figure 1

1. INTRODUCTION

The ASME Boiler and Pressure Vessel Code, Section III, Nuclear Power Plant Components, 1977 edition, (here-in-after referred to as the "Code"), requires an evaluation of the stresses in Class 1 piping systems and gives acceptance criteria in the form of allowable stresses or stress ranges.

Piping systems are characterized by (1) there are numerous piping systems in each nuclear power plant, (2) each piping system consists of a complex structure and there are usually a number of complex-shaped products such as tees, branch connections and elbows in each piping system, (3) every product in the piping system is subjected to a complex combination of loadings consisting of internal pressure, moments and thermal gradients, and (4) some of the complex-shaped products used in piping systems are dimensionally standardized.

As the result of the magnitude and complexity of piping systems stress evaluations, along with standardization of some of the products, simplified methods of evaluation have been developed and are now included as part of the Code; in NB-3600 thereof for Class 1 piping systems. These simplified methods use "flexibility factors" and "stress indices" to represent the structural characteristics of the complex-shaped products used in the piping systems. Flexibility factors are used in the analysis of the piping system; this analysis gives the moment loads acting on each and every portion of the piping system. The moments obtained from the piping system analysis are then used in Code equations and criteria to determine if a particular piping system is acceptable. For example, Equation (10) in NB-3653.1 of the Code is:

$$S_n = C_1 \frac{P_o D_o}{2t} + C_2 \frac{D_o}{2I} \overline{M} + \frac{E\alpha |\Delta T_1|}{2(1-\nu)} + C_3 E_{ab} \, |\alpha_a T_a - \alpha_b T_b| \leq 3S_m \qquad (1)$$

Equation (1) involves stress indices C_1, C_2, and C_3; pressure loading P_o in the first term, moment loading $\overline{M}$ in the second term and thermal gradient loadings in the last two terms. The value of S_n is the sum of these four terms, the Code Criteria* is that $S_n \leq 3S_m$, where S_m is the Code-tabulated

---

* An alternative procedure is provided for $S_n > 3S_m$.

allowable stress intensity for the material at the Code-defined temperature.

At present, the simplified procedures, flexibility factors and stress indices are such that over-estimate of the stresses is anticipated. Such a design process is usually labeled as being "conservative" and it is so from the viewpoint of evaluation of stresses. However, in a broader sense, a "conservative" evaluation of one aspect of design does not necessarily lead to increased reliability of piping systems. For example, failure to meet Equation (1) might lead the designer to increase the length of the piping system so as to increase its flexibility and thus decrease $\overline{M}$. However, this increased length means that there is more pipe, girth welds, and elbows in the piping system; all of which provide additional potential failure locations compared to a piping system evaluated on a more accurate basis. Accordingly, there is a need for more accurate evaluation rather than simply a conservative stress evaluation.

The report is concerned with a type of piping product that is used in many piping systems; i.e. a butt-welding elbow made in accordance with ANSI Standard B16.9 (elbows with $R/r \cong 3$) or ANSI Standard B16.28 (elbows with $R/r \cong 2$). The flexibility factors and stress indices now given in the Code are based on a theory which ignores the effect of whatever may be welded to the ends of the elbow and, in a more subtle sense, the effect of variations in moments through the elbows; for brevity, we hereinafter refer to this theory as NEE-theory (No End Effects theory). The present Code equations are:

$$k = 1.65/h \tag{2}$$

$$C_2 = 1.95/h^{2/3} \tag{3}$$

We seek herein to develop more accurate representations of flexibility factors and stress indices for such elbows.

The elastic characteristics of a curved pipe, subjected to moment loading, may be quite different than indicated by beam theory. This difference between a curved pipe and a curved beam is due to distortions in the plane of the cross section. In 1911, Th. Von Karman[1] published a theoretical analysis of a curved pipe subjected to in-plane moment. Since then, numerous authors[2-15] have expanded and refined the elastic theory in various ways, including out-of-plane bending and combinations of both in-plane and out-of-plane bending with internal pressure. These theories all contain the assumption that all cross sections taken along the arc of the elbows deform indentically. Obviously, this assumption is not valid at the end sections where the elbow is attached to pipe or to a relatively rigid structure such as a flange, valve or pressure vessel nozzle; nor is the assumption valid when two 90° elbows are welded together in an "S" shape and subjected to in-plane moment.

Much of the theoretical work on elbows is based on energy methods in which the distorted cross section is described by a Fourier series of the form $w = \Sigma\, a_n \sin n\,\phi$, where w is the radial displacement of the cross section and ϕ is the coordinate angle around the circumference. The values of a_n are then obtained by minimization of the energy and equating that minimized energy to the known energy of the applied moment. Conceptually, the energy method can be extended to include end-effects by describing the variation in cross section shape as a function of location along the elbow. Thailer and Cheng[16] developed such an analysis method applicable to the specific case of 180° elbows with end constraints. In principle, this approach could be applied to other end-conditions; e.g. attached pipe legs, other kinds of end-restraints, other elbows (90°, 45°, etc.). However, other than the paper by Thailer and Cheng, no published results of this kind of approach are known.

General purpose finite element programs have been developed over the past few years which have the capability of establishing the elastic characteristics of elbows including "end-effects". However, for routine design of piping systems, it is usually not feasible to run a finite-element analysis of each elbow. What is needed, for routine design, are relatively simple design relationships which the designer can use either by hand calculation or by insertion into his piping system analysis computer program. Such simple design equations can be developed by conducting a parametric evaluation of a class of elbows/end

effects; then select the most significant results and fit those results to relatively simple design equations. Such a parametric study was conducted, using the finite element computer program EPACA[17]; it is the purpose of this report to present the most significant results of that parametric study and to develop relatively simple design equations which account for end effects on elbows with arc angles of 45°, 90°, and 180°, with R/r = 2 or 3, and with a "long" straight pipe attached to both ends of the elbow. This, of course, is not the total range of the end-effects problem but is deemed to cover a major application area.

There are at least two papers which contain results of studies on elbows using finite-element analysis; References (18) and (19). However, these contain only a few specific cases and do not provide a basis for development of simple design guidance. A recent paper by Ohtsubo and Watanabe[20] gives the results of a parametric study of 90° elbows with R/r = 2 and 3; with straight pipe attached to the elbow ends. That study was conducted with a special type of finite element; i.e., ring elements.

Tests[7, 9, 10, 21-25] on elbows to determine stresses and flexibility have mostly been conducted on 90° and 180° elbows with attached straight pipe. While, as shown by the finite-element results presented herein, we would not expect much end-effects with respect to maximum stresses and flexibility factors in these tests, the test results did show that stresses and flexibility factors were somewhat less than predicted by the usual "no-end-effects" theories.

Design guidance for elbows given in industrial piping codes and in the ASME Nuclear Power Plant Components Code for Class 2 and 3 piping is based on fatigue tests reported by Markl[24]. While the design guidance does not* include end-effects of the type considered herein, the basic test data given by Markl includes a quite direct indication of end effects of the type considered herein. Markl ran a series of fatigue tests on elbows with the only variable being the elbow arc angle, α_o. The arc angles tested were 180° (a U-bend), 135°, 90°, 75°, 60°, 45°, and 15°. All elbows were welded to straight pipes

---

* There is design guidance for elbows with flanges attached directly to one or both ends of the elbow, but this kind of end restraint is not the subject of this report.

with pipe length of about 5 times the elbow/pipe cross section radius. Markl correlated his tests by the equation $S_f = i\ S_n$, where S_f is the fatigue-effective stress; i is the fatigue-effective stress intensification factor, arbitrarily taken as unity for a typical girth butt weld in straight pipe, and S_n is the nominal stress.

His results for this series of tests were:

α_o, deg.	i-factor		Fatigue Failure Location
	In-Plane	Out-of-Plane	
180	2.02	2.07	Elbow
135	2.10	1.95	↓
90	1.90	1.52	
75	1.70	1.45	
60	1.53	1.32	
45	1.36	1.29	
30	1.28	1.39	Pipe-to-elbow weld
15	1.46	1.63	" " " "

Markl observed that for α_o of 90° and larger, the i-factor was about constant and about equal to that anticipated by no-end-effects theory. However, for 75°, 60°, and 45° elbows, the i-factor decreased in a consistent manner. It is the arc angle effect which is the main aspect of this report. Markl noted that for arc lengths of 30° and 15°, the failures occurred at the welds, not in the body of the elbow as expected by theory, and that the i-factor increased for small α_o. He attributed this to the interaction between the two closely spaced welds and, indeed, the welds for $\alpha_o = 15^o$ were only about three wall-thicknesses apart.

2. SCOPE

This report is concerned with the development of more accurate representations of the flexibility factors and stress indices for butt welding elbows with R/r of 2 or 3 and with "long" straight pipe attached to both ends of the elbow. To accomplish this, a parametric study was conducted using the finite element computer program EPACA[17].

Chapter 3 contains a brief description of the finite element models. Chapter 4 discusses the validation of the models and computer program for the specific application herein.

Chapter 5 contains examples of detailed stress distributions, both in the circumferential and longitudinal directions. Chapter 5 also includes tables of maximum stresses (in the form of stress indices); these are used in Chapter 7 to develop relatively simple but more accurate equations for stress indices. Stresses at welds are also tabulated in Chapter 5 and discussed further in Chapter 8.

Chapter 6 contains a discussion of how the flexibility factors were derived from the finite-element (FE) calculations and includes tables of calculated flexibility factors. These are used in Chapter 7 to develop relatively simple but more accurate equations for flexibility factors.

Chapter 7 discusses the development of relatively simple but more accurate equations for stress indices and flexibility factors and contains recommendations for an addition to the Code to implement these new equations.

Chapter 8 contains a discussion of stresses at the girth butt welds between straight pipe and elbows.

3. FINITE ELEMENT MODELS

The general arrangement of the models is shown in Figure 1*. The dimensions of all models are shown in Table 1*.

Figure 1, solid lines, illustrates a model with $\alpha_o = 90^o$, dashed lines indicate the arrangement for models with $\alpha_o = 45^o$ and 180°. All models consist of an elbow with pipe attached to both ends and ring flanges attached to the pipe ends. The reference surface radius r is 10 inches for all models. The wall thickness t, given in Table 1, is for both the elbow and attached pipes.

The numbers of circumferential elements used in the models are shown in Table 1. For in-plane moment loading, symmetry conditions are such that only one-half of the assembly (ϕ from -90 to +90 degrees) was modeled. The longitudinal spacing of the elements is indicated by the entries under "Rows of Elements" in Table 1.

Boundary conditions consisted of complete fixity of the right-hand end of the models. The left-hand end was loaded at the node points to obtain the static equivalent of in-plane moment M_i or out-of-plane moment, M_o.

---

* Figures and Tables are included in numerical order following the text of the report.

4. VALIDATION OF FINITE ELEMENT MODEL

Before conducting the parametric study using EPACA, it was necessary to decide upon two details of the models:

(a) Appropriate straight pipe lengths (L in Figure 1). It was desirable to make L sufficient so that the flanges/boundary conditions would not significantly affect the calculated stresses near or in the elbows. Such models represent actual piping systems where the pipe is long enough to to be (in-so-far as elbow characteristics are concerned) infinite in length.

(b) Element spacing, both in the longitudinal and circumferential direction. The NEE-theory indicated that the rate of change of stress with ϕ is quite rapid for small λ, less so for large λ; accordingly closer circumferential spacing was used for small λ. The rate of change of stress with α was expected to be slow; longitudinal spacing was selected so that the ratio of length-to-width of the elements was not excessive; the aspect ratio corresponding to the selected node spacings ranges from 1.5 to 4.0.

These decisions were, of course, influenced by cost considerations. The aim was to use as few elements as possible and still obtain good results.

In order to check out the decisions, an analysis was made of an elbow which was tested with in-plane moment loading at ORNL[28]. The parameters of the model, which are essentially those of the test assembly, were as follows:

λ	0.214
R/r	2.80
α_o	90 degrees
R	15 inch
t	0.390 inch
L	21 inch
t_f	2.75 inch
r_f	10.75 inch
Number of Circ. Elements	24 (12 in the half-model)
Rows of elements	
Elbows	9
Pipes	7 (each leg)

Figure 2 shows how the calculated stresses at $\alpha = 45^{\circ}$ from the FE-theory (solid lines) compare with the experimentally-determined stresses obtained from strain gages at $\alpha = 45^{\circ}$. It is apparent that the agreement between test and FE-theory is very good. Similar good agreement was obtained at other α = constant sections.

Figure 2 also shows calculated stresses from the NEE-theory (dashed lines). It can be seen that the agreement with test data is not as good as it is for the FE-theory (solid lines).

The test data versus FE-theory comparison served to check out boundary condition assumptions and element spacing as well as satisfactory performance of the EPACA computer program for this specific application.

5. STRESSES

In-Plane Moment

The maximum calculated stresses are summarized in Table 2. The variation in stress as a function of the circumferential location angle ϕ for Model No. 5 at the cross section $\alpha = 35^{o}$ is shown in Figures 3 and 4. These figures also show the stresses obtained from the NEE-theory.

It can be seen in Figures 3 and 4 that the FE-theory gives lower maximum stresses than the NEE-theory ($-10.25\ S_n$ versus $-12.03\ S_n$) and shifts the stress pattern slightly toward the $\phi = -90$ location; i.e. toward the crotch of the elbow.

It can be seen that the stress varies rapidly with ϕ in the region of peak stresses whereas the circumferential element spacing is 10°. Accordingly, the FE-theory may not have picked up the maximum stress. To adjust for this aspect, interpolations were made between elements in the vicinity to obtain σ_{mi}. These interpolated stresses are summarized in Table 3.

For $\lambda \leq 0.30$, it can be seen in Table 3 that the FE-theory and NEE-theory agree (except for the slight shift in ϕ) as to the maximum stress direction, surface and location. However, for large values of λ, the FE-theory predicts higher maximum stresses than the NEE-theory. It should be noted that large values of λ also involve heavy-wall cross sections; i.e. r/t is 4.19 for $\lambda = 0.75$ and r/t is 2.10 for both $\lambda = 1.00$ and 1.50. Shell theory would not be expected to give accurate evaluations for these heavy-wall cross sections.

For $\lambda \leq 0.3$, it may be noted that models with $\alpha_o = 45^{o}$ show large decreases in maximum stresses as compared to NEE-theory. However, the change in stress magnitude with change in α_o from 90° to 180° is relatively small and the maximum stresses for $\alpha_o = 180^{o}$ remain significantly below the NEE-theory. This suggests that the NEE-theory may overpredict maximum stresses by about 10%, quite independent of end-effects. This may be due to the assumption in the NEE-theory that $R/r \gg 1$, for example see Reference (8).

Figure 5 shows the variation of stress along the ϕ = constant line containing the maximum calculated stress. These data are for Models 4, 5, and 6 along $\phi = -5^{o}$; the stress is in the circumferential direction on the inside surface. Figure 5 illustrates the substantial reduction in maximum stress in the 45° elbow due to the end-effects of the attached pipe. Figure 5 also

illustrates the small difference in maximum stress between a 90° elbow and a 180° elbow, suggesting that the NEE-theory overpredicts maximum stress (for small λ), quite independent of end effects.

Figure 6 is analogous to Figure 5, except it is for Models 22, 23, and 24. For these models, the maximum stresses occur on the $\phi = -81^{\circ}$ line (the nearest element to $\phi = -90^{\circ}$) and are in the longitudinal direction on the outside surface. It should be recalled that these models involve a very heavy-wall cross section; i.e. $r/t = 2.10$. The location $\phi = -81^{\circ}$ is essentially aligned with the maximum compressive nominal stress, σ_n. By thin-wall-shell theory, $\sigma_n = M/(\pi r^2 t)$, hence $\sigma_n/S_n = -1.0$. However, if we simply adjust σ_n by the ratio of the outside radius to the mean radius, we obtain $\sigma_n/S_n = 1.0 \times (12.385/10) = -1.2385$. Applying this same adjustment to the NEE-theory leads to the dashed line shown in Figure 6. With this adjustment, the NEE-theory agrees with the FE-theory as to the direction, surface and location of the maximum stress; i.e. it is a longitudinal stress on the outside surface at $\phi = -90^{\circ}$.

In real piping systems, there will ordinarily be a girth butt weld at the juncture of the elbow with the pipe. For some design work, it may be usefull to know the maximum stress at these welds so that they can be combined with other stress factors for the welds. Review of the detailed calculated results indicates that the maximum stress at the weld essentially occurs along the same ϕ-line containing the maximum calculated stress. Table 4 summarizes the stresses at the welds along the ϕ-line containing the maximum calculated stress. This table will be discussed further in Chapter 8.

Out-of-Plane Moment

The maximum calculated stresses are summarized in Table 5. The variation in stress as a function of the circumferential location angle ϕ for Model 5 at the cross section $\alpha = 35^{\circ}$ is shown in Figures 7 and 8. These figures also show the stresses obtained from the NEE-theory. For out-of-plane moment, the results obtained from the NEE-theory are a function of α because the out-of-plane moment applied to one end of the elbow changes to a torsional moment at the opposite end of the elbow. At $\alpha = 35^{\circ}$, the out-of-plane moment is $\cos 35^{\circ}$ times the applied out-of-plane moment.

It can be seen in Figures 7 and 8 that the FE-theory gives lower maximum stresses than the NEE-theory ($-5.98\ S_n$ versus $-7.98\ S_n$) and shifts the stress pattern.

As for in-plane moment, interpolations were made between elements in the vicinity of the element with the maximum calculated stress to obtain estimates of the maximum stress, σ_{mi}. These interpolated stresses are summarized in Table 6.

Table 5 shows changes in signs of the maximum stress and changes of ϕ-location. However, as can be seen in Figure 7, for circumferential stresses, there are two locations of high inside surface stresses; one at about $\phi = 200^o$ where the stress is tension and one at about $\phi = 340^o$, where the stress is compression. The FE-theory results waver between these two locations for models with $\alpha_o = 45^o$, 90°, or 180°.

Figures 9, 10, and 11 show the variation in circumferential stress as a function of longitudinal location in models 4, 5, and 6, respectively. These data are along the ϕ-lines containing the maximum calculated stress; i.e. along $\phi = 205^o$, 335°, and 205° for Models 4, 5, and 6, respectively. The NEE-theory is also shown in these figures.

For 90° elbows, as indicated in Figure 10, there is an "inverse" end effect in that the circumferential stress at $\alpha = \alpha_o = 90^o$ is not zero; as would be indicated by the NEE-theory. For 180° elbows, there is a reversal in the sign of the out-of-plane moment. This leads to an antisymmetry about $\alpha = 90^o$ which was accurately reflected by the FE-theory for large λ but only approximately for small λ. For example, in Model 6 the stress was the same magnitude, opposite sign, to four significant figures but for Model 24 the stress at $\alpha = 22.5^o$ was $+ 6.577S_n$ whereas the stress at $\alpha = 157.5^o$ was $-5.823S_n$. This presumably reflects the fact that the two sets of end-conditions are not entirely equivalent.

6. FLEXIBILITY FACTORS

In-Plane Moment

To obtain flexibility factors for the elbows, one first needs to obtain displacements and rotations of one end of the model with respect to the other end. As indicated in Figure 1, one end of the model is "fixed" so we can obtain the needed information directly from the displacements and rotations at the "loaded-end" flange node points.

Figure 12 shows the x-direction (see Figure 1) displacements, δ_x, for Model 5, plotted against $\sin\phi$. If the flange rotated as a rigid body, then the values of δ_x would fall in a straight line. It can be seen in Figure 12 that this is almost the case; the slight bowing of the flange is not significant with respect to flexibility factors.

The average δ_x is -3.746×10^{-2} inches. The rotation θ_z can be obtained by taking the difference between δ_x at $\phi = -90^o$ and $\phi = +90^o$, and dividing that difference by 2r; e.g. for Model 5, $\theta_z = (.0680 - .0050)/20 = 3.15 \times 10^{-3}$ radians (at S_n = 1000 psi). A check of this rotation can be made against the average of the θ_z rotations of the nodes on the loaded flanges; these vary from 2.81×10^{-3} to 3.52×10^{-3} radians, with an average of 3.15×10^{-3} radian. (The variation in θ_z is another indication that the loaded flange is not acting like a rigid body.) The other significant displacement, for in-plane moments, is δ_y; this is obtained from the average of the δ_y displacements of the nodes on the "loaded" flange. The remaining displacement, δ_z, and two rotations, θ_x and θ_y, should be zero from symmetry conditions. The FE-theory results are satisfactory in this respect in that, while not zero, they are much smaller than the significant displacement/rotations. For example, for Model 5

$$\delta_x = -3.746 \times 10^{-2} \qquad \theta_x = 2.667 \times 10^{-7} \ (0)$$

$$\delta_y = -1.890 \times 10^{-1} \qquad \theta_y = 2.490 \times 10^{-4} \ (0)$$

$$\delta_z = -1.683 \times 10^{-4} \ (0) \qquad \theta_z = 3.153 \times 10^{-3}$$

However, for this example, we note that θ_y (which should be zero) is about 8% of θ_z; indicating that small errors are present in the FE-theory results. Table 7 summarizes the average values of the significant displacements/rotations δ_x, δ_y and θ_z.

In order to compare the flexibility of the elbows with that obtained from NEE-theory, we assume that the flexibility is uniform throughout the elbow;

the significance of this assumption will become apparent in the following discussion. We also assume that the flanges act as rigid bodies and that the pipe legs contribute to the overall displacement by the nominal relationships; e.g. $\theta = ML/EI$. With these assumptions, flexibility factors can be calculated using the equations shown in Table 8. The resulting flexibility factors are shown in Table 7.

As shown in Table 7, the three flexibility factors k_x, k_y, and k_z are slightly different from each other. The NEE-theory, which assumes that the flexibility of the elbow is uniform over its length, leads to a single flexibility factor for δ_x, δ_y, and θ_z. However, when end-effects are included, three different flexibility factors emerge. For k_z, which indicates the rotation of one end of the elbow with respect to the other end, it doesn't make any difference how the flexibility varies through the elbow because each slice of the elbow contributes equally to the total rotation. However, for displacements, each slice of the elbow contributes differently to the overall displacements. To obtain an "exact" result, we would need to know the flexibility of each slice, $d\alpha$, of the elbow as a function of α and include that function as a part of the integration process. This is a refinement which would lead to very complex design procedures and is not deemed to be worth the added complexity.

For most piping systems, the rotational flexibility factor k_z is of primary importance*. It can be seen in Table 7 that k_z derived from FE-theory follows a consistent pattern; it is always less than k_z obtained from the NEE-theory but approaches the NEE-theory k_z as α_o increases from 45° to 180°

Out-of-Plane Moment

As for in-plane moments, we obtain the appropriate data from the displacements and rotations at the "loaded end" flange node points. Figure 13 shows the x-directions (see Figure 1) displacements, δ_x, for Model 5 plotted against $\cos\phi$. If the flange rotated as a rigid body, then these values of δ_x would fall in straight lines. It can be seen in Figure 13 that this is almost

* The displacement flexibility factors would be significant only where the elbow or elbows constitute a major portion of the entire piping system. Usually, the elbows are attached to pipe with lengths significantly greater than $R\alpha_o$, in which case the local displacements δ_x and δ_y are insignificant.

the case; however there is some slight bowing of the flange.

The rotation θ_y can be obtained by taking the difference between δ_x at $\phi = 0$ and $\phi = 180^o$ and dividing that difference by 2r; e.g. for Model 5, $\theta_y = (.01797 + 0.01797)/20 = 1.797 \times 10^{-3}$ radians (at $S_n = 1000$ psi). A check of this rotation can be made against the average of the θ_y rotations of the nodes on the "loaded" flange; these vary from 1.27×10^{-3} to 2.24×10^{-3} radian, with an average of 1.800×10^{-3} radian. (The variation in θ_y is another indication that the loaded flange is not acting as a rigid body.)

For out-of-plane moment, δ_x, δ_y and θ_z should be zero. The FE-theory is satisfactory in this respect in that, while not zero, they are much smaller than the significant displacements/rotations of δ_z, θ_x and θ_y. For example, for Model 5:

$$\delta_x = -9.224 \times 10^{-5} \quad (0) \qquad \theta_x = 9.950 \times 10^{-4}$$

$$\delta_y = 4.405 \times 10^{-5} \quad (0) \qquad \theta_y = 1.800 \times 10^{-3}$$

$$\delta_z = 1.132 \times 10^{-1} \qquad \theta_z = 6.955 \times 10^{-6} \quad (0)$$

Table 9 summarizes the average values of the significant displacements/rotations of δ_z, θ_x and θ_y.

In order to compare the flexibility of the elbows with that obtained from NEE-theory we assume, as for in-plane bending, that:

(1) The flexibility is uniformly distributed throughout the elbow.

(2) The flanges act as rigid bodies

(3) The pipe legs displace/rotate by the nominal relationships.

For out-of-plane bending, however, a pure out-of-plane moment exists only in the loaded pipe and at $\alpha = 0$ of the elbow; for $\alpha > 0$ there is a combination of out-of-plane and torsional moment acting on the elbow. We assume that the incremental rotation for an elbow section under torsional moment is given by the nominal relationship: $d\theta = M_t R d\alpha / GJ$, where G = shear modulus and J = polar moment of inertia = $2\pi r^3 t$. With these assumptions, flexibility factors can be calculated using the equations shown in Table 10.

As indicated in Table 10, a value of k_y for $\alpha_o = 180^o$ cannot be obtained because, under the assumptions made, the value of θ_y is zero. As can be seen in Table 9, by FE-theory the value of θ_y is small and essentially negligible.

As shown in Table 9, the three flexibility factors (two for $\alpha_o = 180^o$) are slightly different from each other. These differences presumably reflect the end-effects plus variation of the moment from M_o at $\alpha = 0$ to $M_o \cos\alpha$ and $M_t \sin\alpha$ for $\alpha > 0$.

For most piping systems, the rotational flexibility is of primary importance. For out-of-plane moment we have two such rotational flexibility factors, k_x and k_y. In subsequent evaluation in Chapter 8, we will use the average of k_x and k_y. It may be noted that, unlike k_z for in-plane moment, the values of k_x and k_y do not increase monotonically as α_o increases. There are apparently balancing influences; for $\alpha = 45^o$, the end-effects of the straight pipe are large but M_o persists throughout the elbow while for $\alpha_o = 180^o$, the end-effects of the attached pipe are relatively small but M_o is converted to M_t at $\alpha = 90^o$ and to $-M_o$ at $\alpha = 180^o$.

7. DESIGN GUIDANCE

The parametric study made using EPACA provides a basis for introducing relatively simple but more accurate design procedures than now in the Code. These must be described as "relatively" simple because they are necessarily more complex than the present method of the Code where $C_2 = 1.95/h^{2/3}$ and $k = 1.65/h$; quite independent of any end effects.

Maximum Stresses

In-Plane Moment

Figure 14 shows maximum stresses from Table 3 as a function of the parameter h, along with the straight line labeled $C_2 = 1.95/h^{2/3}$. The equation $C_2 = 1.95/h^{2/3}$ (but not less than 1.5) is at present a part of NB-3600 of the Code. It is used to calculate stresses by the equation:

$$\sigma = C_2 \frac{D_o}{2I} \overline{M} \tag{4}$$

where D_o = outside diameter of the elbow cross section, I = section modulus of the elbow cross section and $\overline{M} = [M_i^2 + M_o^2 + M_t^2]^{1/2}$. Figure 14 may be considered as investigating the accuracy of equation (4) for the particular condition where $M_o = M_t = 0$.

It should be noted that $S_n = M/\pi r^2 t$ hence the line represented by $C_2 = 1.95/h^{2/3}$ is not precisely the same as the Code equation (4) herein. It is essentially the same for $r/t > 10$. However, the points plotted at h = 0.95 and 1.43 are for models with r/t = 2.1. For r/t = 2.1, the ratio of $(D_o/2I)/(1/\pi r^2 t)$ is 1.171. This essentially compensates for the stresses that are above the line $C_2 = 1.95/h^{2/3}$.

Figure 14 indicates that maximum stresses for 90° and 180° elbows are not significantly reduced by the end-effects of the attached pipe. However, for 45° elbows, a significant reduction in maximum stress occurs. The line labeled $C_2 = 1.75/h^{.56}$ is recommended for 45° elbows, with linear interpolation on α_o permitted for α_o between 45° and 90°.

Extrapolation of the data would indicate that elbows with $\alpha_o < 45^o$ could be assigned still lower stress indices. We do not have any FE-theory for $\alpha_o < 45^o$ but we do have a theoretical aim point; $C_2 = 1.0$ at $\alpha_o = 0$. It is recommended that this extrapolation be permitted to $\alpha_o = 30^o$.

In summary, it is recommended that for in-plane bending:

$$C_2 = 1.95/h^{2/3} \text{ for } \alpha_o \geq 90°$$

$$C_2 = 1.75/h^{.56} \text{ for } \alpha_o = 45°$$

$$C_2 = 1.0 \text{ for } \alpha_o = 0$$

Linear interpolation with α_o is to be used, but C_2 shall not be less than interpolated for $\alpha_o = 30^o$ and not less than 1.0 for any α_o.

Figure 15 shows examples of the proposed design equations, along with the FE theory data points. Figure 15 also shows curves taken from Reference (27). Reference (27) states that the data on which their curves are based were obtained from a general three-dimensional thin shell finite element program. Specifically, the curves shown in Figure 15 are from Figure 3 of Ref. (27), which gives ratios of the maximum circumferential stress to the nominal stress, S_n.

The FE-theory data points, while not at exactly the same h-value as Ref. (27) theory, agree quite well with Ref. (27) curves except at $\alpha_o = 180°$. It should be recalled that for $\alpha_o = 180°$, the design equations are simply the NEE theory. That the maximum stress in 180° elbows is <u>greater</u> than obtained from NEE theory is deemed to be implausible, hence, we doubt the validity of those portions of Ref. (27) curves which are above the design equations. At small values of α_o, Ref. (27) curves go to zero, as they should. However, our design equations encompass the maximum stress in any direction, and for small α_o, the longitudinal stress is larger than the circumferential stress, hence the theoretical stress index is not less than 1.0 even for very small α_o. Also, our design equations for $\alpha_o < 30°$ contain a judgemental margin for possible adverse effects of two closely-spaced girth butt welds (see discussion on p. 5).

Except at large values of α_o, the data from Ref. (27) serves to confirm the results obtained from the FEE theory parametric study. Ref. (27) covers only in-plane moments. As a further source of confirmatory data, we have reviewed

the results given by Ohtsubo and Watanabe[20], which covers both in-plane and out-of-plane bending but only 90° elbows. The results from Ref. (20) also are in reasonably good agreement with the results of the FEE theory parametric study.

Out-of-Plane or Torsional Moments

Figure 16 shows maximum stresses from Table 6 as a function of the parameter h, along with the straight line labeled $C_2 = 1.95/h^{2/3}$. Figure 16 may be considered as investigating the accuracy of Equation (4) for the particular condition where $M_i = 0$.

Figure 16 indicates that there are relatively small differences as a function of α_o. There are apparently balancing effects; for $\alpha_o = 45^o$, the end-effects of the straight pipe are relatively large but M_o persists through the elbow while for $\alpha_o = 180^o$ the end-effects of the straight pipe are relatively small but M_o is converted to M_t at $\alpha = 90^o$ and to $-M_o$ at $\alpha = 180^o$. However, Figure 16 indicates that for all α_o, the maximum stress is significantly less* than indicated by Equation (4). The straight dashed line shown in Figure 16 labeled $C_2 = 1.71/h^{.53}$ is deemed appropriate to represent these results.

These results represent stresses due to combinations of M_o and M_t, normalized to $S_n = M_o/\pi r^2 t$. For a given value of M_o and α_o, M_t is simply $M_o \sin \alpha_o$. However, our calculations only cover those conditions where $M_o/M_t \geq 1.0$. We have not covered the case where $M_o/M_t < 1.0$; this relationship can exist for elbows with $\alpha_o < 90^o$. As an extreme example, there could be an "elbow" with $\alpha_o = 5^o$, subjected to a unit value of M_t on one end; for this case $M_t = 1.0$, $M_o = 0.087$. We wish to cover loadings where M_o/M_t is less than unity as well as those where M_o/M_t is equal to or greater than unity; the latter is the condition for which we have calculated results.

The common assumption is that the shear stress in an elbow due to M_t is just the same as in straight pipe; i.e.

$$\tau = \frac{1}{2} \frac{D_o}{2I} M_t \quad . \tag{5}$$

* As discussed for in-plane bending, the difference between $D_o/2I$ and $1/\pi r^2 t$ compensates for values shown in Figure 16 at h = 0.95 and 1.43.

Because the Code limits stress intensities and stress intensity is equal to 2τ, Equation (5) can be written

$$\sigma = 1.00 \frac{D_o}{2I} M_t \quad . \tag{6}$$

We have no evidence, from the present work, that Equation (6) is valid but it seems almost certain that it is. If so, then we would expect that if we apply to an elbow a combination of M_o and M_t such that $M_t > M_o$, and normalized the stress to $S_n = M_t/\pi r^2 t$, we would expect maximum values of σ_{mi}/S_n to be equal to or less than obtained in the Finite Element calculations for $M_o/M_t > 1.0$ and by the correlation equation of Figure 16; $C_2 = 1.71/h^{.53}$. Accordingly, the maximum stress can be calculated by the equation:

$$\sigma_o = C_2 \frac{D_o}{2I} M_o \tag{7}$$

where M_o is the out-of-plane moment at $\alpha = 0$ and $C_2 = 1.71/h^{.53}$. Figure 16 directly indicates the accuracy of Equation (7) where $M_o > M_t$; we would expect Equation (7) to over-estimate stresses where $M_o < M_t$.

Flexibility Factors

In-Plane Moment

Figure 17 shows the rotational flexibility factors, k_3, from Table 7 plotted against the parameter h. The line labeled $k = 1.65/h$ is the NEE-theory flexibility factor for small ($< \sim 1.0$) values of h. The line in Figure 17 labeled $k = 1.10h$ represents the flexibility factors for $\alpha_o = 45°$. The line in Figure 17 labeled $k = 1.3/h$ represents the flexibility factors for $\alpha = 90°$.

The finite element results indicate that flexibility factors for $\alpha = 180°$ are about the same as for 90° elbows. Recalling that the flexibility factors represent an integration over the arc length, and that end effects occupy a smaller portion of the arc length in 90° elbows than in 180° bends, we would expect 180° bends to have flexibility factors higher than 90° elbows and approaching the factors given by NEE-theory. Possibly the FE-theory loses its accuracy for large values of α_o because more elements are involved. This

aspect needs further checking but, at this time, our best judgement is that the flexibility factors for 180° bends should be the same as given by NEE-theory. Accordingly, it is recommended that:

$$k = 1.65/h \quad \text{for} \quad \alpha_o \geq 180°$$

$$k = 1.30/h \quad \text{for} \quad \alpha_o = 90°$$

$$k = 1.10/h \quad \text{for} \quad \alpha_o = 45°$$

$$k = 1.00/h \quad \text{for} \quad \alpha_o = 0$$

Linear interpolation is to be used, but k shall not be less than 1.0 for any α_o.

Figure 18 shows examples of the proposed design equations, along with the FE-theory data points. Figure 18 also shows curves taken from Reference (27). The correlations are good except at $\alpha_o = 180°$.

Out-of-Plane Moment and Torsional Moment

Figure 19 shows the average of the rotational flexibility factors, $(k_x + k_y)/2$, from Table 9, along with the straight line labeled $k = 1.65/h$. As remarked earlier, flexibility factors for out-of-plane moment are not a monotonic function of α_o. The dashed line labeled $k_o = 1.25/h$ represents an average value for an out-of-plane flexibility factor, k_o. It is recommended that this be used for out-of-plane moments.

Noting that the values of flexibility factors shown in Table 9 were derived using $d\theta = M_t R d\alpha/GJ$, it is appropriate to assign a flexibility of 1.00 for torsional moments.

Recommended Code Rules

The preceding recommendations are summarized in the form of a recommended addition to footnote 8 to Table NB-3683.2-1. For this purpose, we change to the moment definitions of footnote 5 to Table NB-3683.2-1; i.e. $M_i = M_2$, $M_o = M_1$, and $M_t = M_3$. The recommended addition reads as follows:

Alternatively, for butt welding elbows per ANSI B16.9, MSS SP87, or ANSI B16.28, the limits of Equations (9) through (14) may be checked by replacing those terms containing M_i or M_i^* with terms given in (c) and (d), provided:

(a) the elbows are welded on both ends to straight pipes of the same nominal thickness as the elbow and the length of those straight pipes is not less than two times the nominal outside diameter of the elbow.

(b) In conducting the piping system analysis (NB-3672.6), the flexibility factors for elbows used in the analysis are:

$$k_1 = 1.65/h \text{ for } \alpha_o \geq 180°$$

$$k_1 = 1.30/h \text{ for } \alpha_o = 90°$$

$$k_1 = 1.10/h \text{ for } \alpha_o = 45°$$

$$k_1 = 1.0 \text{ for } \alpha_o = 0$$

Linear interpolation with α_o shall be used for α_o between 180° and 0°, but k_1 shall not be less than 1.0.

$$k_2 = 1.0$$

$$k_3 = 1.25/h, \text{ but not less than } 1.0$$

where

k_1 = flexibility factor for moment M_1

k_2 = flexibility factor for moment M_2

k_3 = flexibility factor for moment M_3

α_o = arc angle (degrees) of the elbow

$h = tR/r^2$.

(c) Replace B_2M_i in Equation (9) with:

$$0.75\ [(C_{22}\ M_2)^2 + (C_{23}\ M_1)^2 + (C_{23}\ M_3)^2]^{1/2} \quad .$$

(d) Replace C_2M_i or $C_2M_i^*$ in Equations (10) through (14) with:

$$[(C_{22}\ M_2)^2 + (C_{23}\ M_1)^2 + (C_{23}\ M_3)^2]^{1/2} \quad .$$

(e) Definitions:

$C_{22} = 1.95/h^{2/3}$ for $\alpha_o \geq 90^o$

$C_{22} = 1.75/h^{.56}$ for $\alpha_o = 45^o$

$C_{22} = 1.0$ for $\alpha_o = 0$.

Linear interpolation with α_o shall be used, but C_{22} shall not be less than interpolated for $\alpha_o = 30^o$ and not less than 1.0 for any α_o.

$C_{23} = 1.71/h^{.53}$, but not less than 1.0.

$h = tR/r^2$

α_o = arc angle (degrees) of elbow .

The definitions of types of loadings given under Equations (9), (11), and (12) apply to the moment components M_1, M_2, and M_3.

Discussion of Recommendations

The limitation in (a) simply reflects the conditions under which the calculations were made. The flexibility factors in (b) and stress indices in (e) are a straightforward presentation of the recommendations previously developed. Calculation of stresses due to combined moments in (d) merits some comment.

Calculations were made using EPACA for M_2 (in-plane moment, M_i), by itself; the expression in (d) reverts back to the calculated results for the special case where $M_1 = M_3 = 0$. Calculations were also made using EPACA for $M_2 = 0$, and combinations of M_1 (M_o) and M_3 (M_t) such that $M_1(\alpha) = M_{1(\alpha=0)}\sin\alpha$. The stresses were indexed to $M_{1(\alpha=0)}$, from which we obtained the C_{23} index. For $M_2 = 0$, the expression in (d) can be written:

$$C_{23}\ (M_1^2 + M_3^2)^{1/2} \tag{8}$$

which is equivalent to:

$$C_{23}\ M_{1(\alpha=0)}\ [\cos^2\alpha + \sin^2\alpha]^{1/2} \quad . \tag{9}$$

Noting that $\cos^2\alpha + \sin^2\alpha = 1.0$, it is apparent that the expression in (d) reverts back to the calculated results for that special case where $M_2 = 0$.

We wish to cover the general case where all combinations of M_1, M_2, and M_3 might be applied to the elbow. We could do this by simply adding the maximum stress due to M_2 to the maximum stress due to M_1 and M_3. However, in general, the maximum stress due to M_2 does not occur at the same location as that due to M_1. An example of this is shown in Figures 3 and 7. The maximum stress due to M_2 (M_i) occurs at $\phi \cong 0$, at which location the stress due to M_1 (M_o) is about zero and, similarly, the maximum stress due to M_1 occurs at $\phi \cong 340^o$, at which location ($\phi = -20^o$), the stress due to M_2 is about zero. Accordingly, we use the statistical mean of the two maximum stresses as a simple approximation. It is believed that this is conservative but a more rigorous check should be made.

At large values of h, the elbow stresses are the same as stresses in equivalent straight pipe. At this bound, we have a longitudinal stress given by $\sigma = (D_o/2I)(M_1^2 + M_2^2)^{1/2}$ and a shear stress given by $\tau = (D_o/4I)M_3$. The expression in (d) is intended to reflect maximum stress intensities due to

moment loading; stress intensity is defined as 2τ. In a stress field consisting of a combination of normal stresses and shear stresses, the maximum stress intensity is given by:

$$\bar{\sigma} = 2\tau_{max} = [\sigma^2 + 4\tau^2]^{1/2} \tag{10}$$

Substituting $(D_o/2I)(M_1^2 + M_2^2)^{1/2}$ for σ and $(D_o/4I)M_3$ for τ we obtain:

$$\bar{\sigma} = \frac{D_o}{2I}(M_1^2 + M_2^2 + M_3^2) \quad . \tag{11}$$

Accordingly, for large $h(C_{22} = C_{23} = 1.0)$, the expression in (d) becomes an exact equation for stress intensity due to a combination of moment loads.

Provision (c) follows the present practice of assigning a "limit load stress index" equal to 0.75 times the elastic stress index.

It may be noted that the proposed stress indices are equal to or less than the present stress indices. From this aspect alone, it may be possible to accept piping systems which might not be acceptable under the present rules. However, the proposed rules require the use of a lower flexibility factor in conjunction with the lower stress indices. The lower flexibility factors, for a given thermal expansion or anchor movement, will result in higher magnitudes of the applied moments. The amount that calculated stresses are changed by the proposed rules depends upon the relative contribution of the elbow or elbows to that of other parts of the piping system.

To illustrate what may happen, let us consider a "piping system" consisting of a 45° elbow with attached straight pipe and subjected to an in-plane rotation, θ_z. The ratio, J, of elbow-to-pipe contribution to end rotation is:

$$J = \frac{k_i R \cdot \pi/4}{2L + k_i R \cdot \pi/4} \quad . \tag{12}$$

Under the proposed rules, $L \geq 4r$. For a specific example, let us consider an elbow with $R/r = 3$, $h = 0.4$. Then $k_i = 1.10/h = 2.75$. Equation (12) then gives a maximum value of $J = 0.447$. The ratio M_{in}/M_{io}, where M_{in} is the in-plane moment by the proposed rules, M_{io} is the in-plane moment by the present rules, is given by:

$$\frac{M_{in}}{M_{io}} = \left(\frac{k_{io}}{k_{in}} - 1\right) J + 1 \qquad (13)$$

where k_{io} and k_{in} are the present and proposed flexibility factors, respectively. The value of J, for this example, is a maximum of 0.447; it could range down to zero as the pipe lengths increase and thus the flexibility contribution of the elbow becomes negligible. Some illustrative values of σ_n/σ_o, where σ_n = stress calculated by proposed rates, σ_o = stress calculated by present rates, are:

J	$\frac{M_n}{M_o}$	$\frac{\hat{C}_{22}}{C_2}$	$\frac{\sigma_n}{\sigma_o}$
.447	1.224	.795	.973
.2	1.100	.795	.875
0	1.000	.795	.795

Accordingly, for this particular example (45° elbow, straight pipe legs, in-plane rotation, R/r = 3, h = 0.4), the more accurate proposed rules will permit acceptance where the present rules might not. However, no generalization can be made, even for static analysis for specified displacements or weight loading. Dynamic analysis cannot be predicted without going through the complete piping system analysis because the change in flexibility factors may significantly change the frequency response.

As a final point in this discussion, it should be noted that the proposed Code addition is an alternative to the present rules. There are two reasons for this. First, the proposed rules, while deemed more accurate than the present rules, are not grossly different than the present rules and their improvement in accuracy, particularly when considering other sources of errors in the evaluation of piping systems, is not a compelling reason to prohibit the present rules. Second, the proposed rules will require changes in existing piping system analysis computer programs and this will take time to implement. The recommended rules, if accepted, would presumably be implemented to evaluate border-line cases which are not quite acceptable under the present rules.

8. STRESSES AT WELDS

Under NB-3600, the intent of the Code is that at least two checks be made of welding elbows; one in the body of the elbow at an α-location that produces maximum stresses as a function of α, the other at one of the two welds which produces the maximum stresses. In evaluating the welds, the procedure is the same as if the weld were between two lengths of straight pipe. In doing this, the stresses due to the interaction between the elbow and straight pipe are, in effect, ignored.

The justification for this procedure stems from the fatigue tests run by Markl[24]; some of his results are cited in Chapter 1. It should be noted that Markl's fatigue tests on elbows automatically include the interactions between stresses at the welds due to the presence of an elbow and the weld discontinuities inherent in the welds he used to attach legs to the elbow. Fatigue failures, for arc angles 45° and larger, occurred in the body of the elbows rather than in the welds. For piping covered by NB-3600 (design temperature below 700F), the room-temperature fatigue tests run by Markl give some assurance that elbow-weld interactions can be neglected. However, with thin-wall stainless steel piping intended for reliable, long time service at elevated temperatures (e.g. LMFBR piping), the interaction effects may not be negligible.

Table 4 shows the stresses at the elbow-to-pipe juncture for both in-plane and out-of-plane moment. It can be seen in Table 4 that the ratio of σ_w/σ_{mc} is almost independent of α_o. Figure 20 shows the averages of σ_w/σ_{mc} for $\alpha_o = 45^o$, 90°, and 180° plotted against h. Simple design guidance can be obtained by using the straight line approximations shown in Figure 20. The designer who is concerned with stresses at the welds can then obtain a reasonable estimate of maximum stresses at the welds by the equations

$$\sigma_w/S_n = [1.95/h^{2/3}][0.76\ h^{.27}] = 1.48/h^{.4} \quad . \qquad (14)$$

Equation (14) is such that σ_w/S_n is equal to unity at essentially the same h-value as required to make $1.95/h^{2/3}$ equal to unity; i.e. $h \cong 2.7$. Use of this "aim point" is deemed appropriate because at $h > 2.7$, the elbow stresses are equal to those in straight pipe and the maximum stress in the weld is the same as in the elbow. The value of σ_w/S_n should not be taken as less than 1.0.

The direction of the maximum stress at the welds is significant. If that maximum stress is in the circumferential direction then it does not directly intensify stresses due to the usual types of weld discontinuities such as root imperfections, weld reinforcement or radial weld shrinkage. However, if the maximum stress is in the longitudinal direction then it does, to some extent, intensify stresses due to the usual types of weld discontinuities. We can establish a rough bound on h for circumferential or longitudinal maximum stresses at the welds from Tables 2 and 5. For $h \leq 0.3$, the maximum stress is circumferential; for $h \geq 0.75$ the stress is usually longitudinal. We have shown this bound at $h = 0.5$ in Figure 20.

It should be noted that Figure 20 indicates that maximum stresses at the welds are in the circumferential direction for $h < 0.5$. However, as illustrated by Figures 3, 4, 7, and 8, the stress in the longitudinal direction is not much less than in the circumferential direction. One notes further in Figures 4 and 8 that the axial stresses are high only for a small portion of the circumference and hence would not necessarily be equivalent to a more general longitudinal stress such as occurs in straight pipe. Further study of the subject of elbow-weld interaction effects and their implication to design of high-temperature, thin-wall piping is needed before any recommendations can be made for Code rules such as those in Code Case 1592.

9. SUMMARY

The finite element computer program EPACA was used in a parametric study of elbows with $R/r = 2$ or 3, $\alpha_o = 45^o$, 90°, or 180° and for $h = tR/r^2$ ranging from 0.048 to 1.43. The elbows were modeled with lengths of straight pipe attached; the lengths were sufficient to simulate an elbow welded to effectively infinite length straight pipe on both ends.

The data obtained from EPACA calculations were used to develop relatively simple but more accurate equations for maximum stresses and flexibility factors; these are contained in Chapter 7 in the form of a recommended alternative method for addition to the Code. The recommended equations for maximum stresses and flexibility factors are in reasonable accord with similar design guidance given in Reference (27).

The data obtained from EPACA calculations was also used to determine the stresses at welds (elbows-to-pipe junctures). The maximum stresses can be estimated by the equation:

$$\sigma_w/S_n = 1.48/h^{.4}, \text{ but not less than } 1.0 \quad .$$

The maximum stress is parallel to the weld for h less than about 0.5, normal to the weld for larger h, where $h = tR/r^2$.

10. REFERENCES

(1) Von Karman, Th., "Uber die Formaenderung duennwandiger Rohre, insbesondere federnder Ausgleichrohre", Zeitschrift des Vereines deutscher Ingenieure, Vol. 55, 1911.

(2) Hovgaard, W., "Deformation of Plane Pipes", J. of Mathematics and Physics, Vol. 7, Oct. 1928.

(3) Vigness, I., "Elastic Properties of Curved Tubes", Trans. ASME., Vol. 65, 1943.

(4) Beskin, L., "Bending of Curved Thin Tubes", Trans. ASME., J. of Applied Mechanics, Vol. 67, 1945.

(5) Clark, R. A., and Reissner, E., "Bending of Curved Tubes", Advances in Applied Mechanics, Academic Press, New York, Vol. 2, 1951.

(6) Symonds, P. S., and Pardue, T. E., "Characteristics of Short-Radius Tube Bends", Second Partial Report (Theoretical), Naval Research Laboratory Report No. 9-2761, 1945.

(7) Gross, N., "Experiments on Short-Radius Pipe Bends", Proc. Inst. Mech. Engrs., Vol. 1B, 1952.

(8) Turner, C. E., and Ford, H., "Examination of the Theories for Calculating the Stresses in Pipe Bends Subjected to In-Plane Bending", Proc. Inst. Mech. Engrs., Vol. 171, 1957.

(9) Kafka, P. G., and Dunn, M. B., "Stiffness of Curved Circular Tubes with Internal Pressure", Trans. ASME J. of Applied Mechanics, Vol. 78, 1956.

(10) Rodabaugh, E. C., and George, H. H., "Effect of Internal Pressure on Flexibility and Stress-Intensification Factors of Curved Pipe or Welding Elbows", Trans. ASME. Vol. 79, 1957.

(11) Smith, R. T., "Theoretical Analysis of the Stresses in Pipe Bends Subjected to Out-of-Plane Bending", J. Mech. Eng'g Science, Vol. 9, No. 2, 1967.

(12) Jones, N., "In-Plane Bending of a Short-Radius Curved Pipe Bend", Trans. ASME, J. of Eng'g for Industry, Vol. 89, 1967.

(13) Cheng, D. H., and Thailer, H. J., "In-Plane Bending of Curved Circular Tubes", Trans. ASME, J. Engr. for Industry, Vol. 90, 1968.

(14) Cheng, D. H., and Thailer, H. J., "On Bending of Curved Circular Tubes", Trans. ASME, J. Engr. of Industry, Vol. 92, 1970.

(15) Dodge, W. G. and Moore, S. E., Stress Indices and Flexibility Factors for Moment Loadings on Elbows and Curved Pipe", Welding Research Council Bulletin No. 179, December 1972.

10. REFERENCES
(Cont.)

(16) Thailer, H. J., and Cheng, D. H., "In-Plane Bending of a U-Shaped Tube With End Constraints", Trans. ASME, J. Engr. for Industry, Vol. 92, 1970.

(17) EPACA, See "Theory and Users Manual For EPACA, General Purpose Finite Element Analysis Program for Three-Dimensional Thick Shell Structures" Available from Argonne Code Center, Argonne National Laboratory, Argonne, Ill.

(18) Davidson, H., and Godino, V., "The Determination of the Flexibility of a Short-Radius Elbow Using Discrete Element Methods", U. S. Naval Marine Engineering Laboratory Contract No. N-161-26198, Electric Boat Company, Report No. EB-U-411-66-030, May, 1966.

(19) Wright, W. B., Rodabaugh, E. C., and Thailer, H. J., "Influence on End-Effects on Stresses and Flexibility of a Piping Elbow with In-Plane Moment", In Pressure Vessels and Piping: Analysis and Computers, June, 1974. Published by ASME, 345 E. 47th St., New York, N.Y. 10017.

(20) Ohtsubo, H. and Watanabe, O., "Flexibility and Stress Factors of Pipe Bends - An Analysis by the Finite Ring Method", Trans. ASME, J. of Pressure Vessel Technology, May 1977.

(21) Vigness, I., "Elastic Properties of Curved Tubes", Trans. ASME, Vol. 65, 1943.

(22) Pardue, T. E., and Vigness, I., "Properties of Thin-Walled Curved Tubes of Short-Bend Radius", Trans. ASME, Vol. 73, 1951.

(23) Findlay, G. E., and Spence, J., "In-Plane Bending of a Large 90° Smooth Bend", J. of Strain Analysis, Vol. 1, No. 4, 1966.

(24) Markl, A.R.C., "Fatigue Tests of Piping Components", Trans. ASME, Vol. 74, 1952.

(25) Imamaza, J. and Uragami, K., "Experimental Study of Flexibility Factors and Stresses of Welding Elbows with End Effects", Second Int'l Conf. on Pressure Vessel Technology, Proceedings, Part 1-30, pp 417-426, ASME 1973.

(26) MSS-SP75(1975 edition), "Specification for High Test Wrought Welding Fittings", Published by Manufacturer's Standardization Society, 1815 North Fort Myer Drive, Arlington, VA 22209.

(27) "Flexibilities of and Stresses in Thin Pipe Bends Under In-Plane Bending: Influence of Bend Angle and Tangent Pipe Ends.", Engineering Sciences Data Unit, ESDU75014, 251-259 Regent Street, London W1R 7AD

(28) Dodge, W. G. and Bolt, S. E., "Experimental Stress Analysis of Machined 10-in. Diameter Pipe Elbows with Specified Geometric Distortions", ORNL/NUREG-36 (To be published)

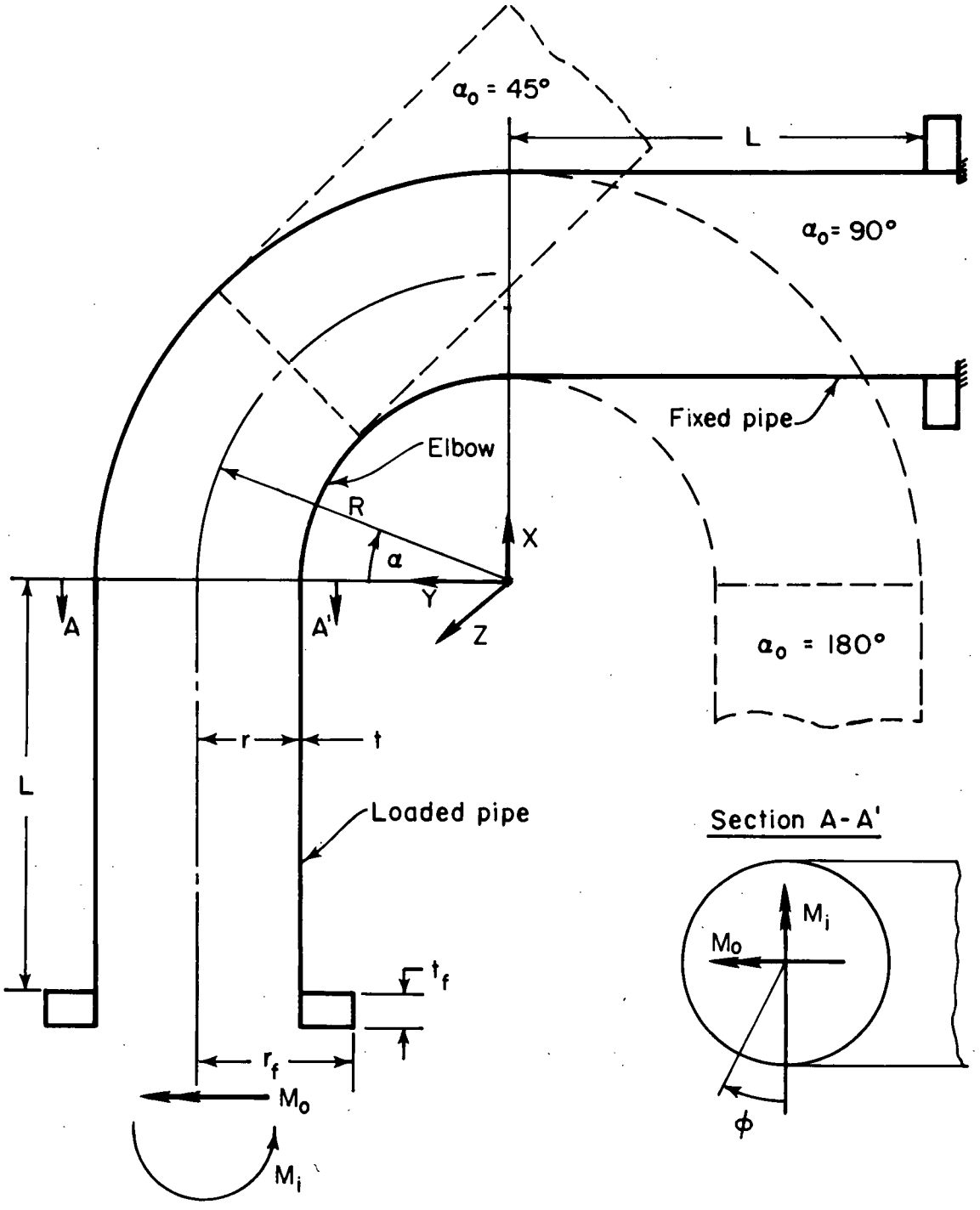

FIGURE 1. FINITE ELEMENT MODEL, See Table 1 for dimensions and element layout

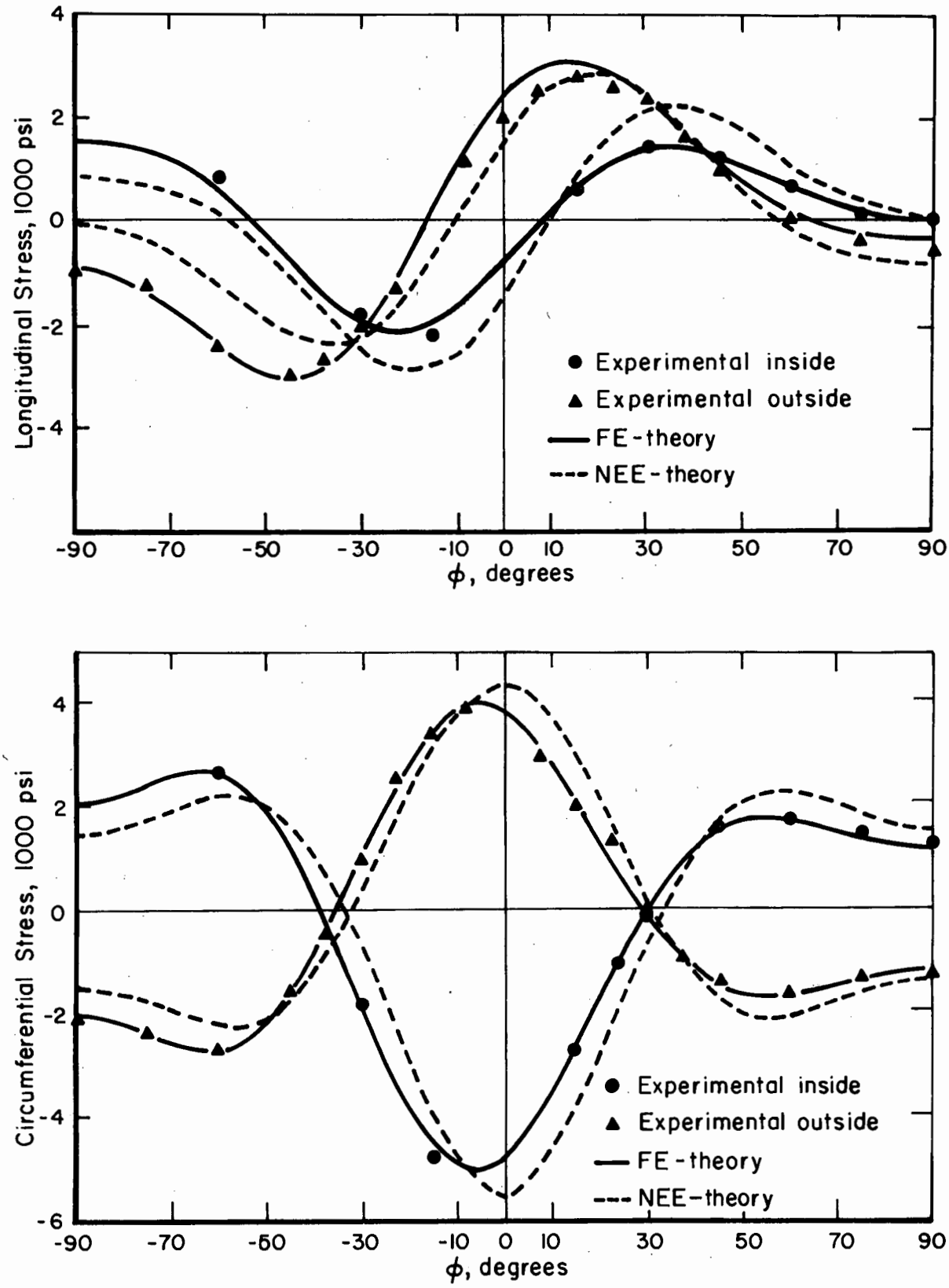

FIGURE 2. COMPARISON OF FE-THEORY WITH TEST DATA, ELBOW WITH λ = 0.214, R/r = 2.80 AND α_o = 90°, IN-PLANE MOMENT

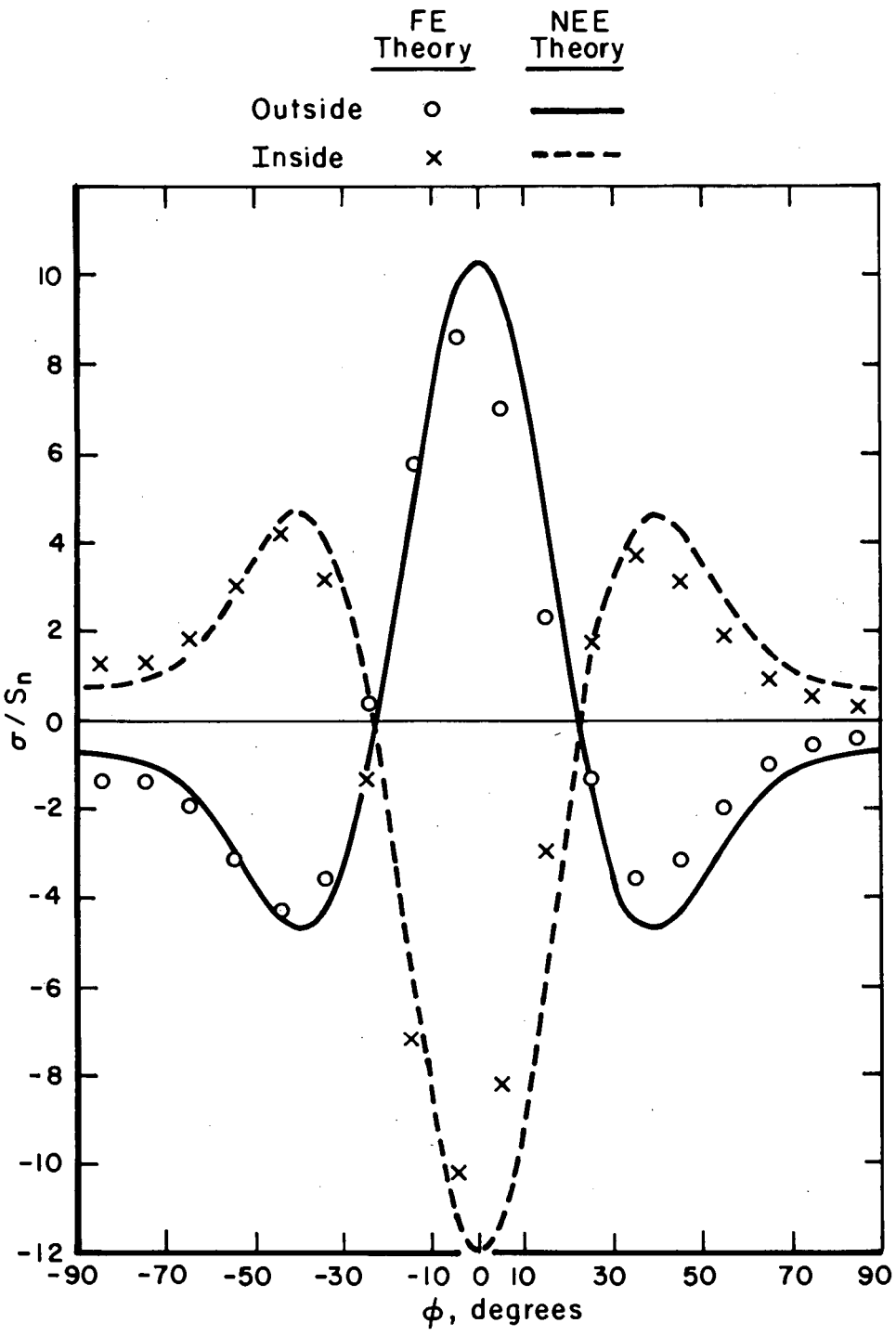

FIGURE 3. IN-PLANE MOMENT, CIRCUMFERENTIAL STRESS AS A FUNCTION OF ϕ, MODEL 5 (λ = 0.075, R/r = 3.0, α_o = 90°), at α = 35°

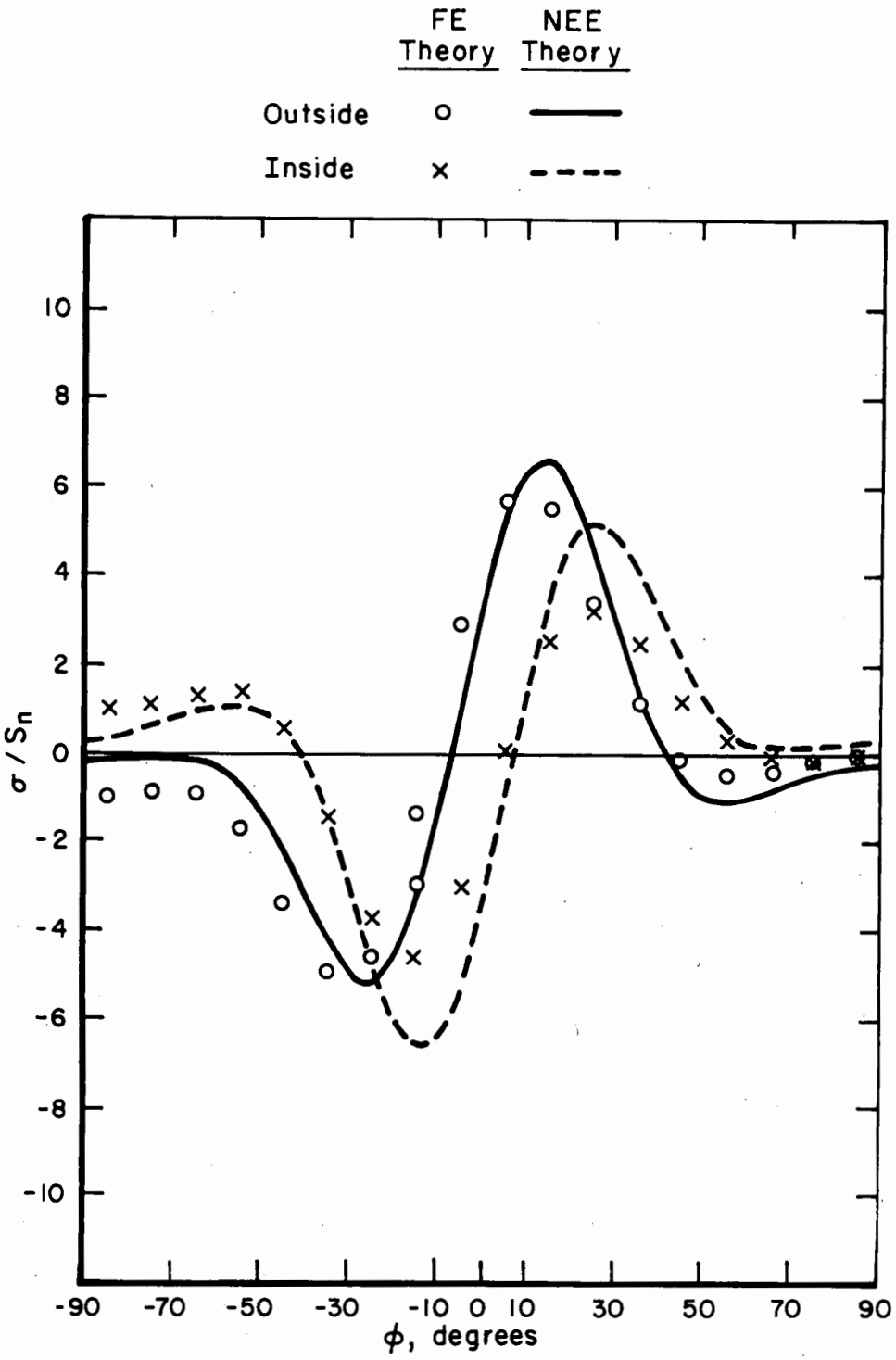

FIGURE 4. IN-PLANE MOMENT, LONGITUDINAL STRESS AS A FUNCTION OF ϕ, MODEL 5 (λ = 0.075, R/r = 3.0, α_o = 90°), at α = 35°.

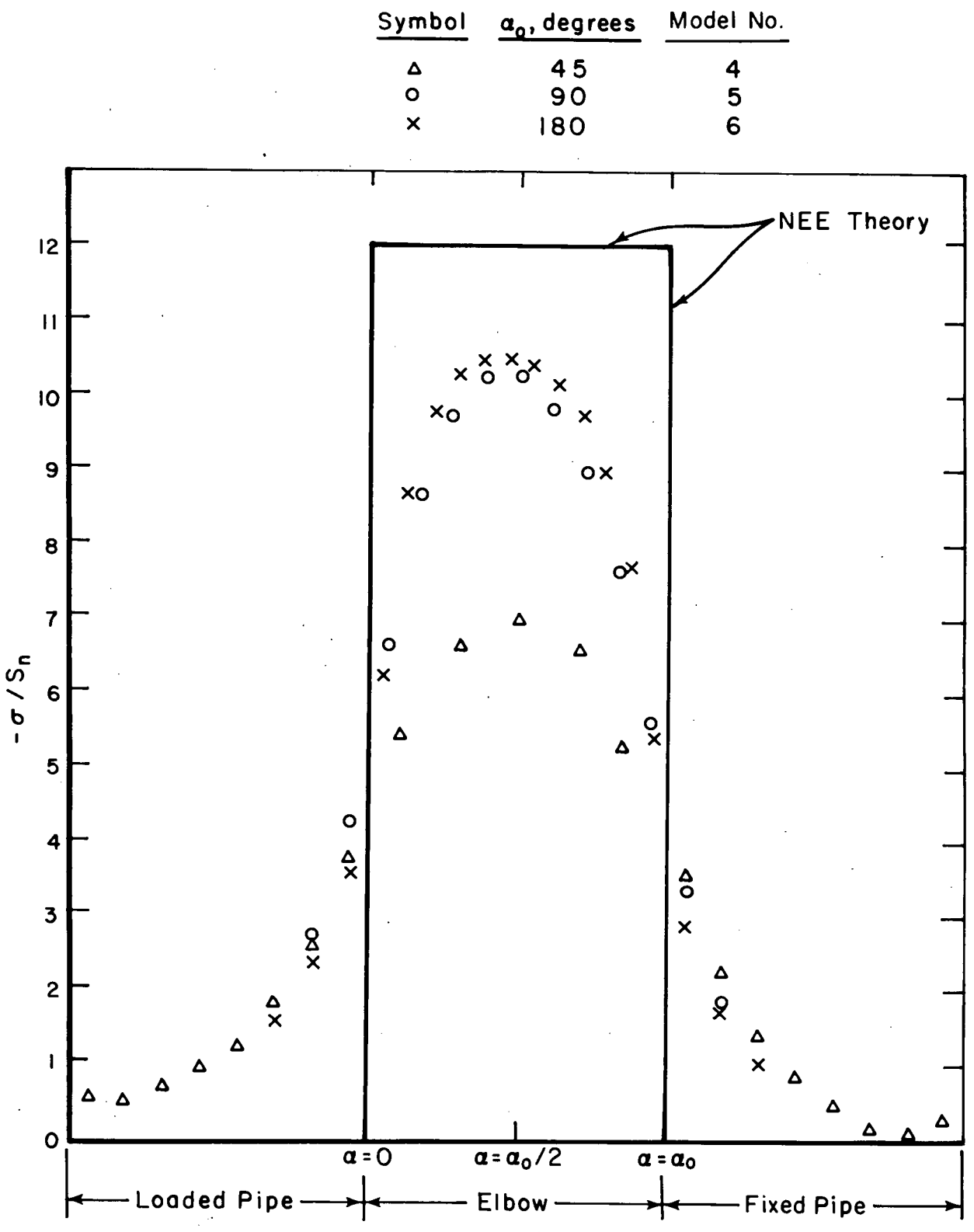

FIGURE 5. IN-PLANE MOMENT, CIRCUMFERENTIAL STRESS AS A FUNCTION OF LONGITUDINAL LOCATION, MODELS 4, 5, AND 6 (λ = 0.075, R/r = 3.0), AT ϕ = -5°

Symbol	α_0, degrees	Model No.
△	45	22
○	90	23
×	180	24

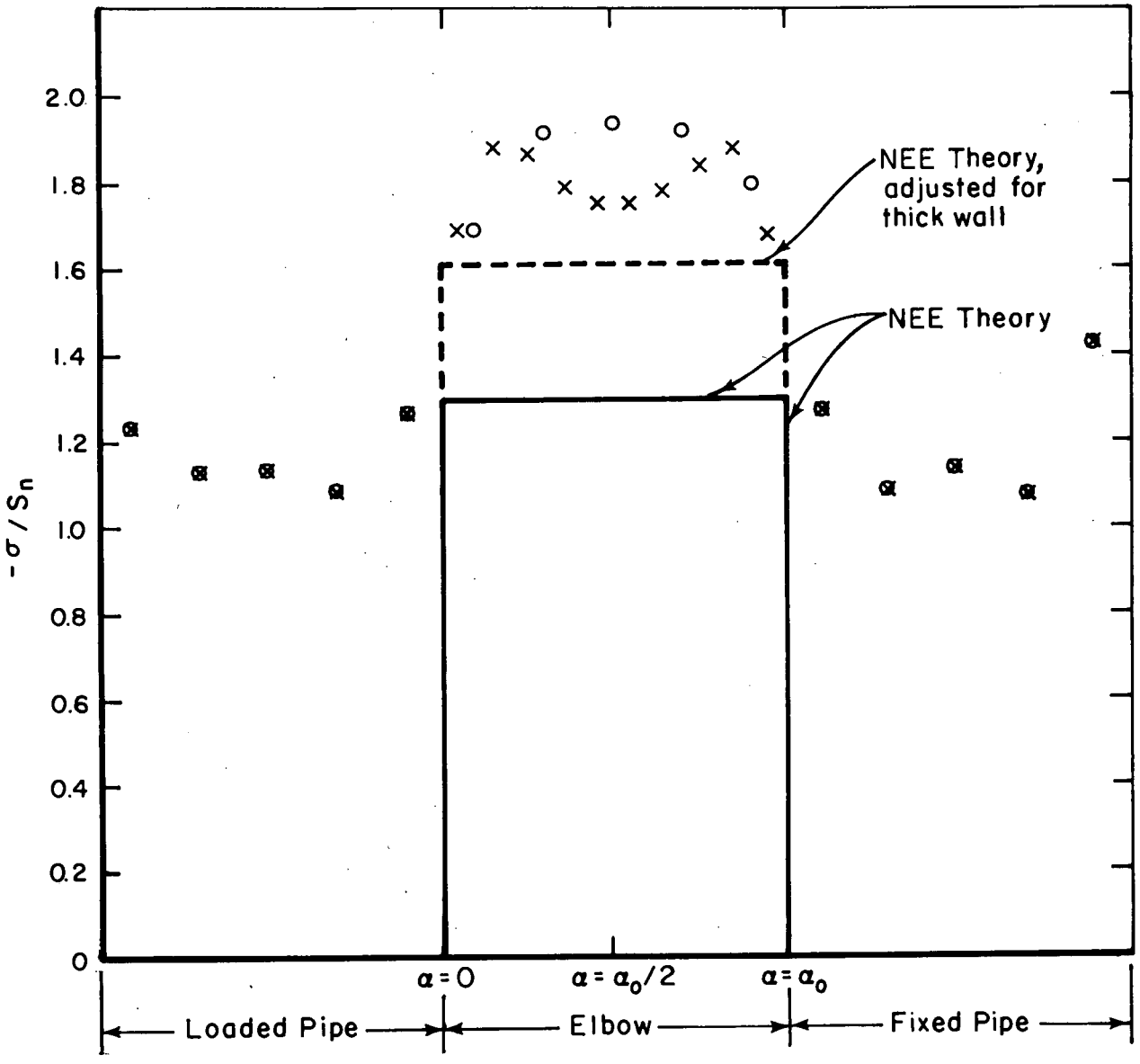

FIGURE 6. IN-PLANE MOMENT, LONGITUDINAL STRESS AS A FUNCTION OF LONGITUDINAL LOCATION MODELS 22, 23, AND 24 (λ = 1.50, R/r = 3.0) at $\phi = -81^{\circ}$

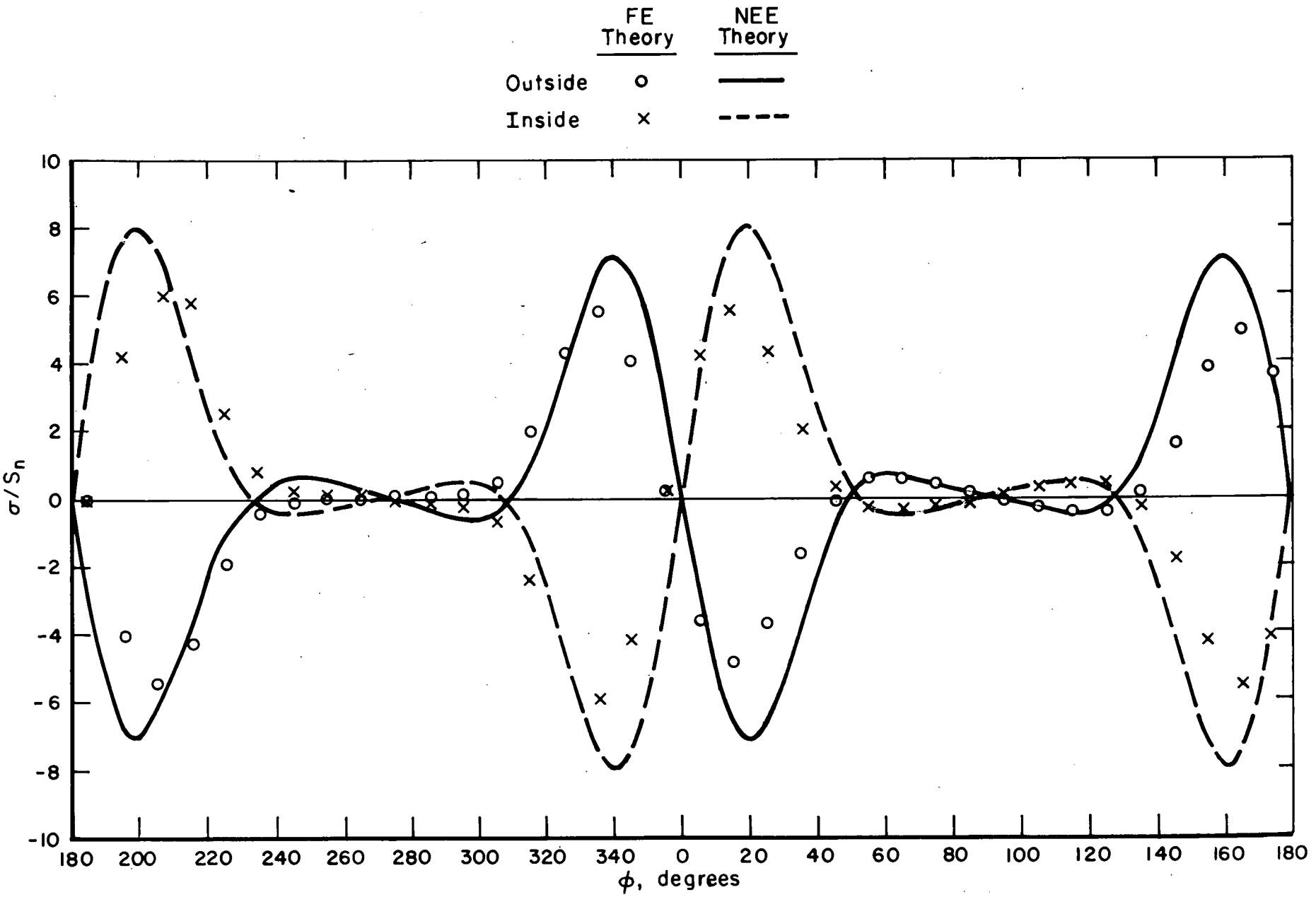

FIGURE 7. OUT-OF-PLANE MOMENT, CIRCUMFERENTIAL STRESS AS A FUNCTION OF ϕ, MODEL 5 (λ = 0.075, R/r = 3.0, α_o = 90°), at α = 35°

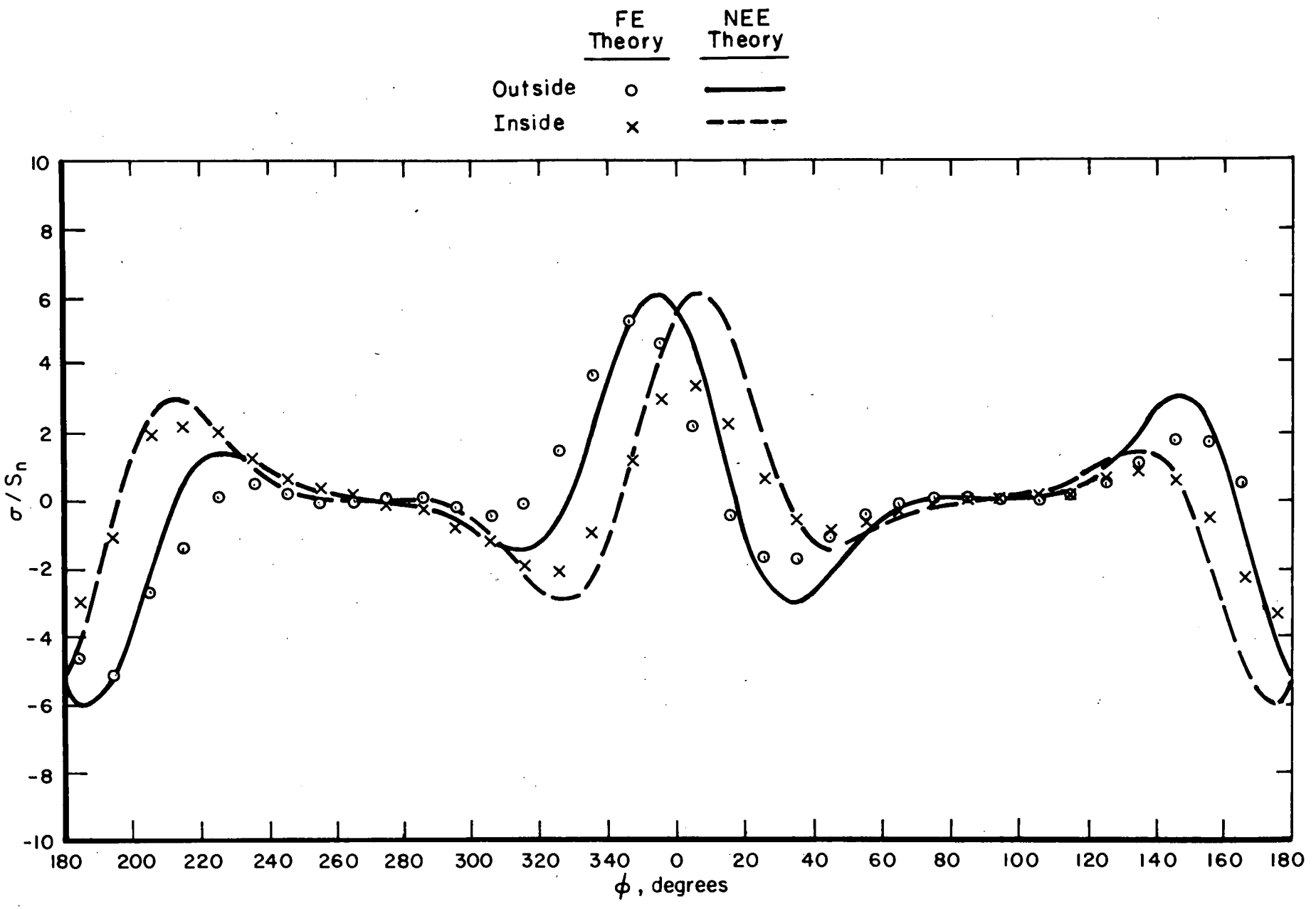

FIGURE 8. OUT-OF-PLANE MOMENT, CIRCUMFERENTIAL STRESS AS A FUNCTION OF ϕ, MODEL 5 (λ = 0.075, R/r = 3.0, α_o = 90°), at α = 35°

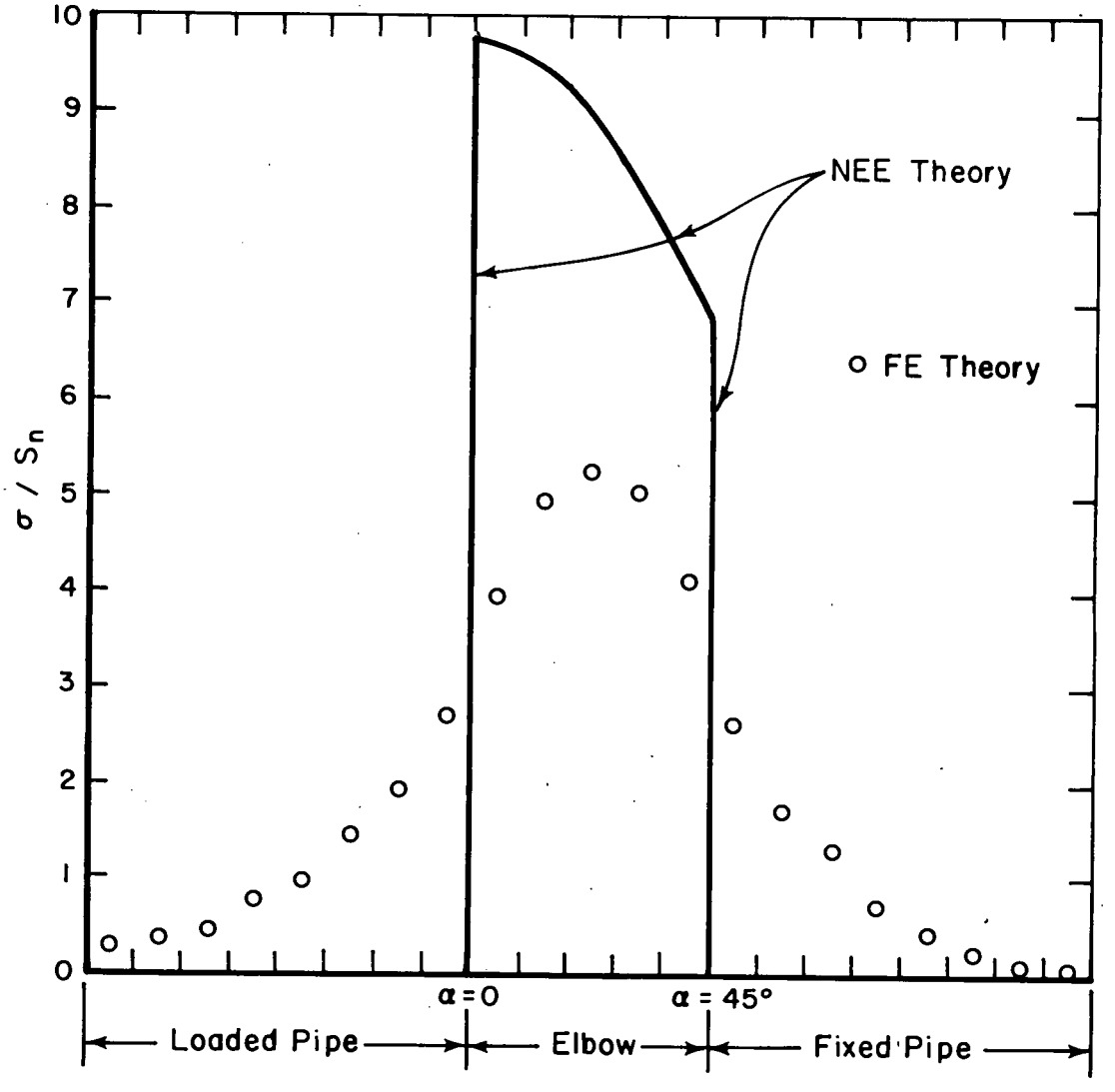

FIGURE 9. OUT-OF-PLANE MOMENT, CIRCUMFERENTIAL STRESS AS A FUNCTION OF LONGITUDINAL LOCATION, MODEL 4 (λ = 0.075, R/r = 3.0, α_o = 45°), at ϕ = 22.5°

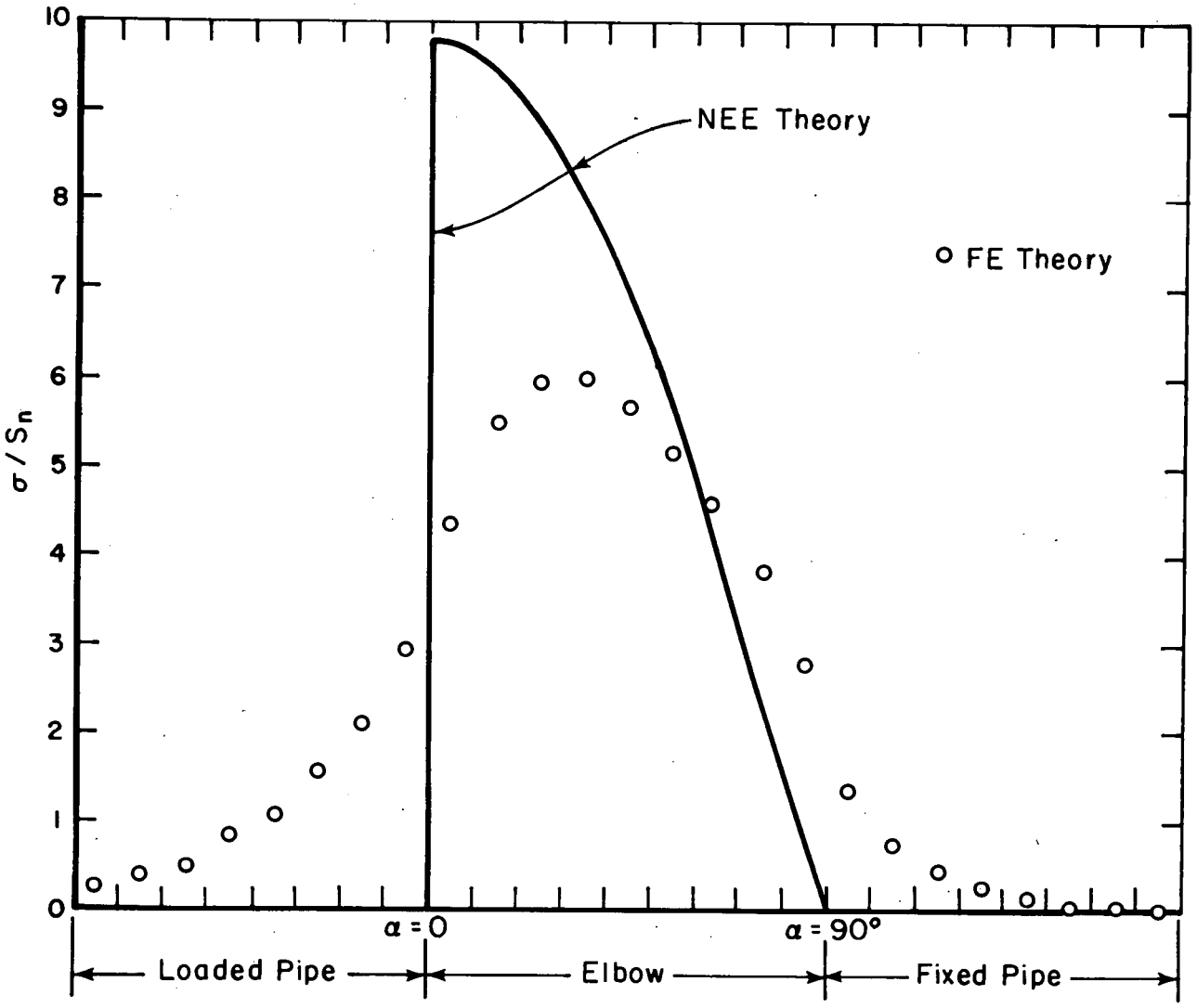

FIGURE 10. OUT-OF-PLANE MOMENT, CIRCUMFERENTIAL STRESS AS A FUNCTION OF LONGITUDINAL LOCATION, MODEL 5 (λ = 0.075, R/r = 3.0, α_o = 90°), AT ϕ = 35°

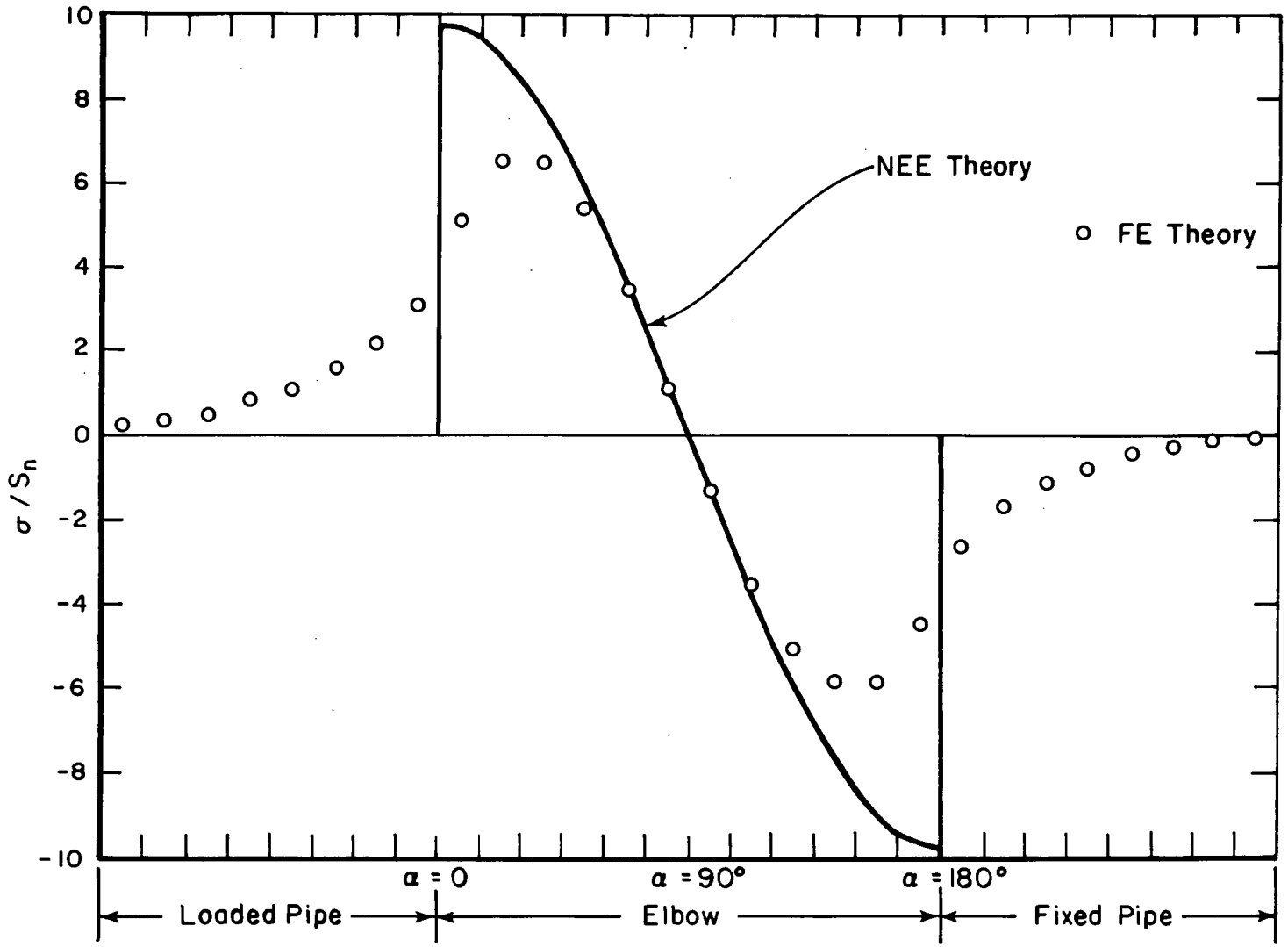

FIGURE 11. OUT-OF-PLANE MOMENT, CIRCUMFERENTIAL STRESS AS A FUNCTION OF LONGITUDINAL LOCATION, MODEL 6 (λ = 0.075, R/r = 3.0, α_o = 180°), at ϕ = 22.5°

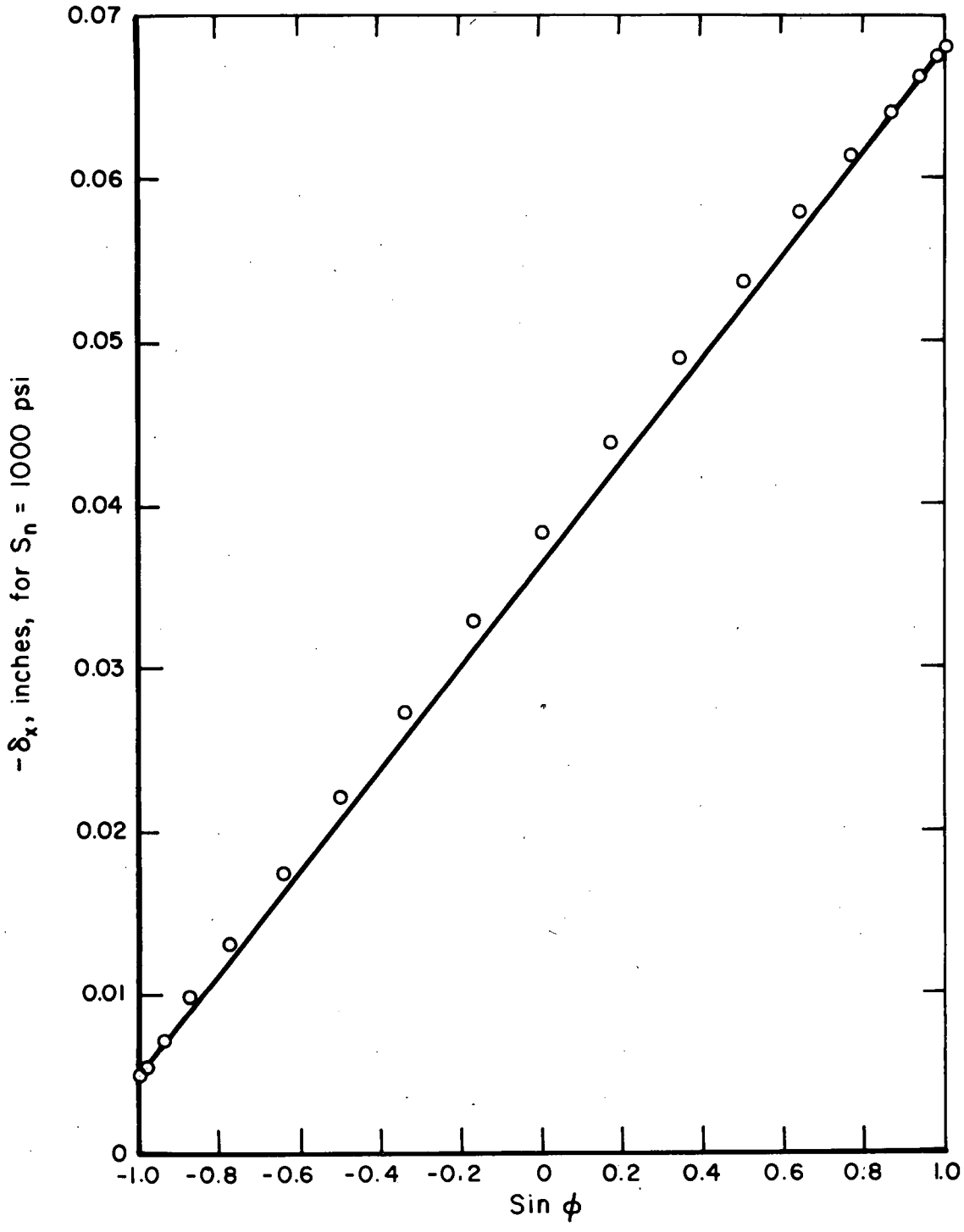

FIGURE 12. ILLUSTRATION OF ESSENTIALLY PLANAR ROTATION OF LOADED-END FLANGE, MODEL 5, IN-PLANE MOMENT, FLEXIBILITY FACTOR CALCULATIONS

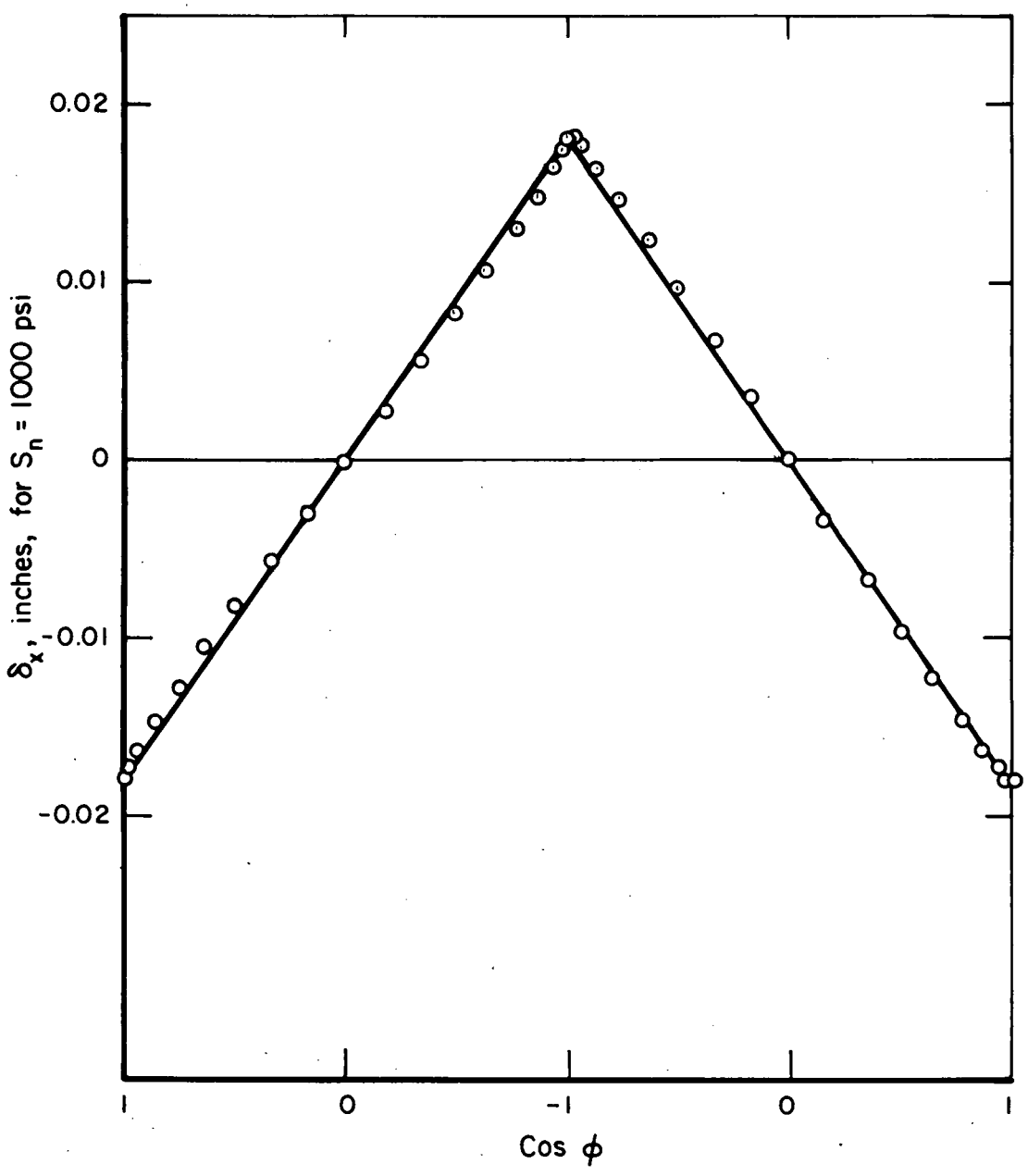

FIGURE 13. ILLUSTRATION OF ESSENTIALLY PLANAR ROTATION OF LOADED-END FLANGE, MODEL 5, OUT-OF-PLANE MOMENT, FLEXIBILITY FACTOR CALCULATIONS

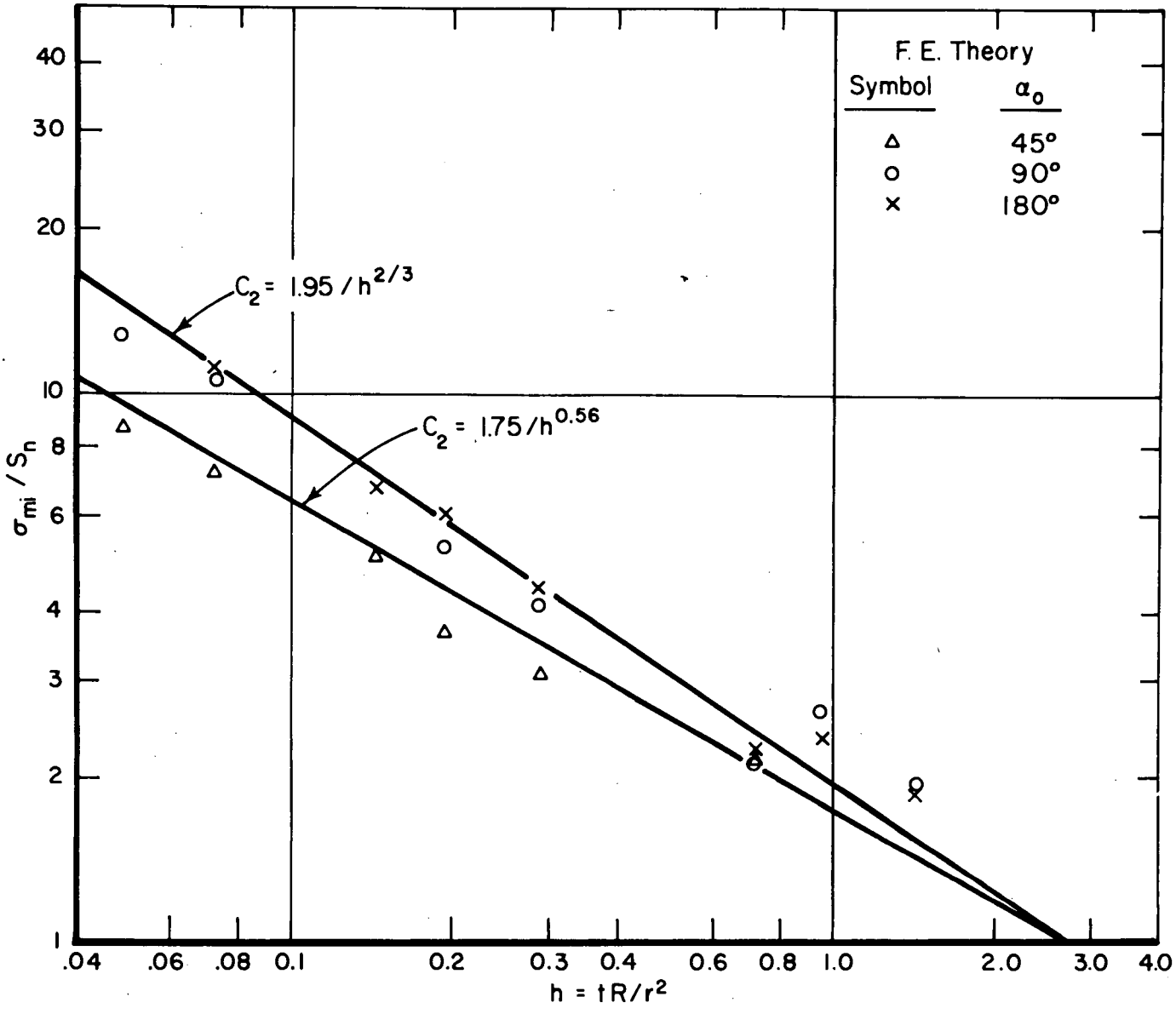

FIGURE 14. IN-PLANE MOMENT, MAXIMUM STRESSES AS A FUNCTION OF h, RECOMMENDED STRESS INDEX EQUATION FOR $\alpha_o = 45°$

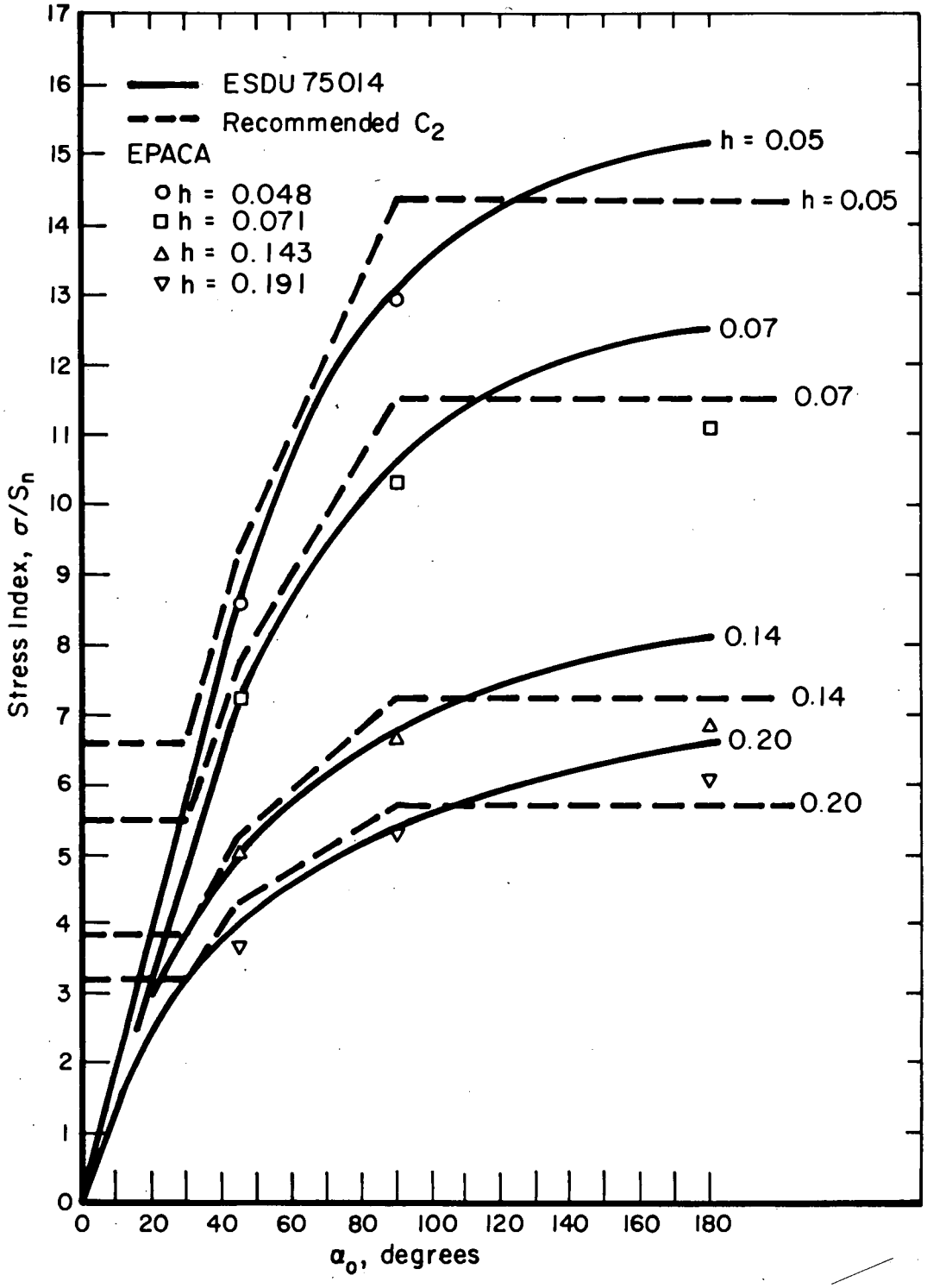

FIGURE 15: COMPARISONS OF MAXIMUM CIRCUMFERENTIAL STRESS INDEX. IN-PLANE BENDING OF ELBOWS WITH PIPE TANGENTS

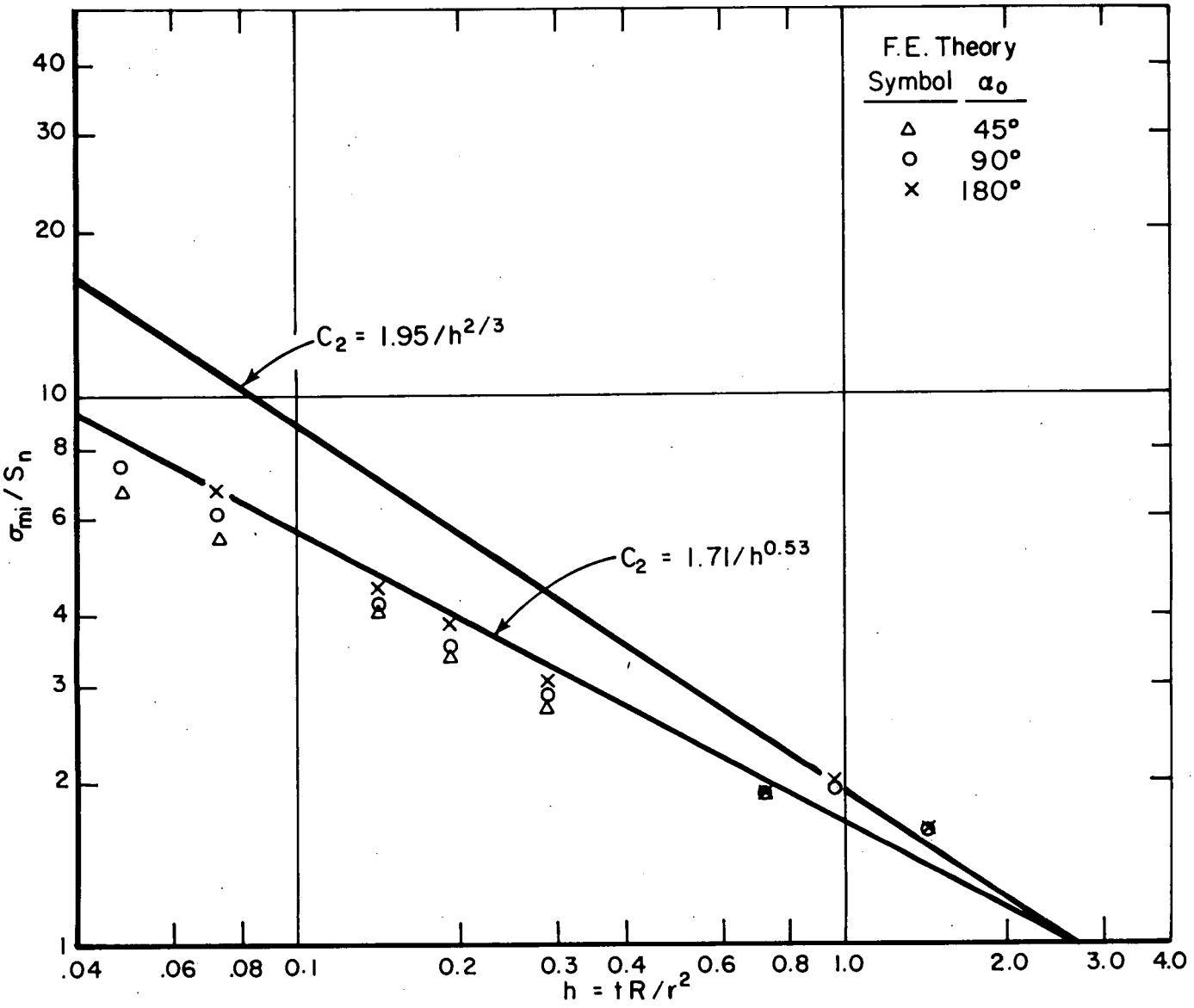

FIGURE 16. OUT-OF-PLANE MOMENT, MAXIMUM STRESSES AS A FUNCTION OF h, RECOMMENDED STRESS INDEX EQUATION FOR ALL α_o

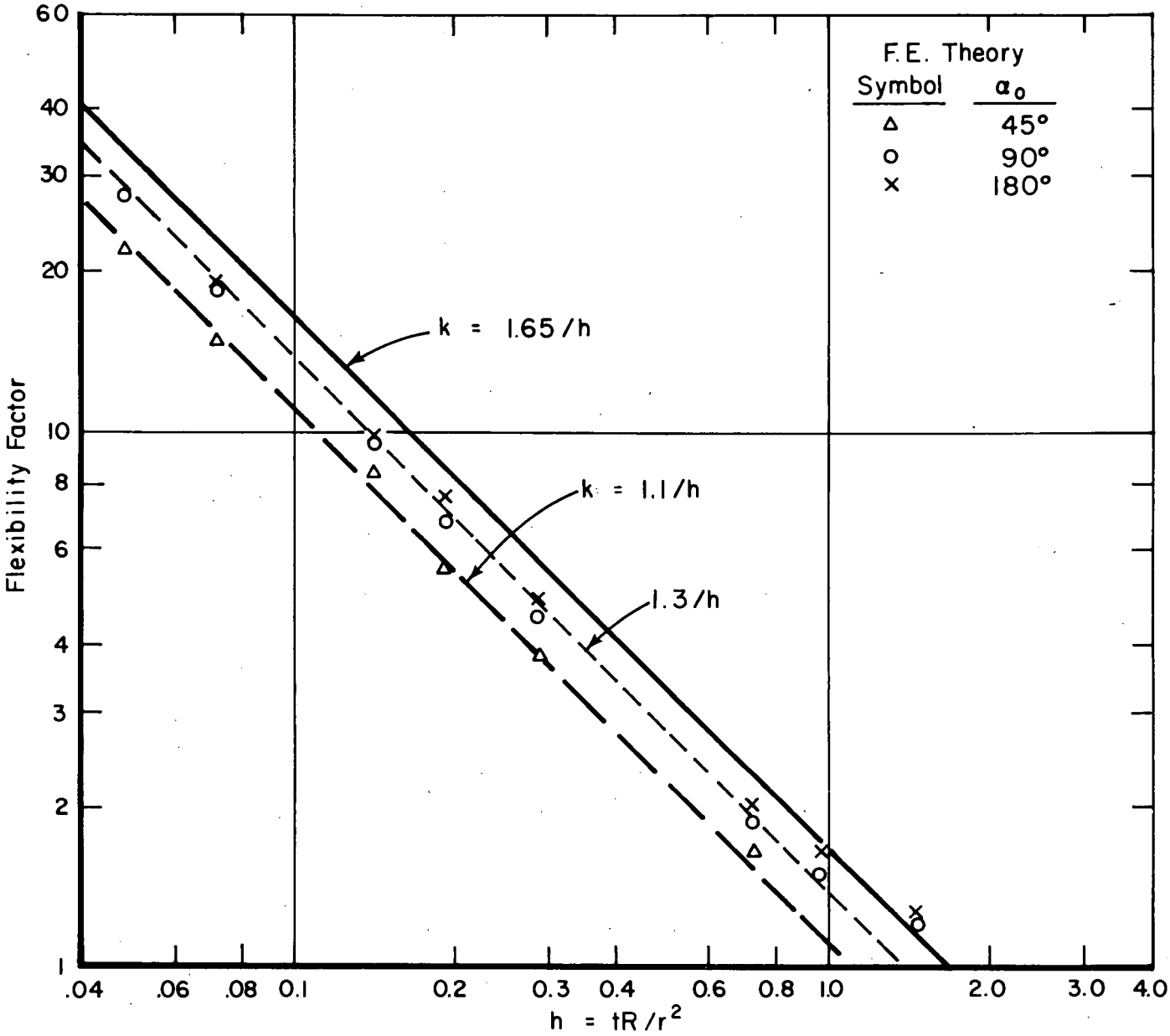

FIGURE 17. IN-PLANE MOMENT, FLEXIBILITY FACTORS AS A FUNCTION OF h, RECOMMENDED FLEXIBILITY FACTOR EQUATION FOR α_o = 45°

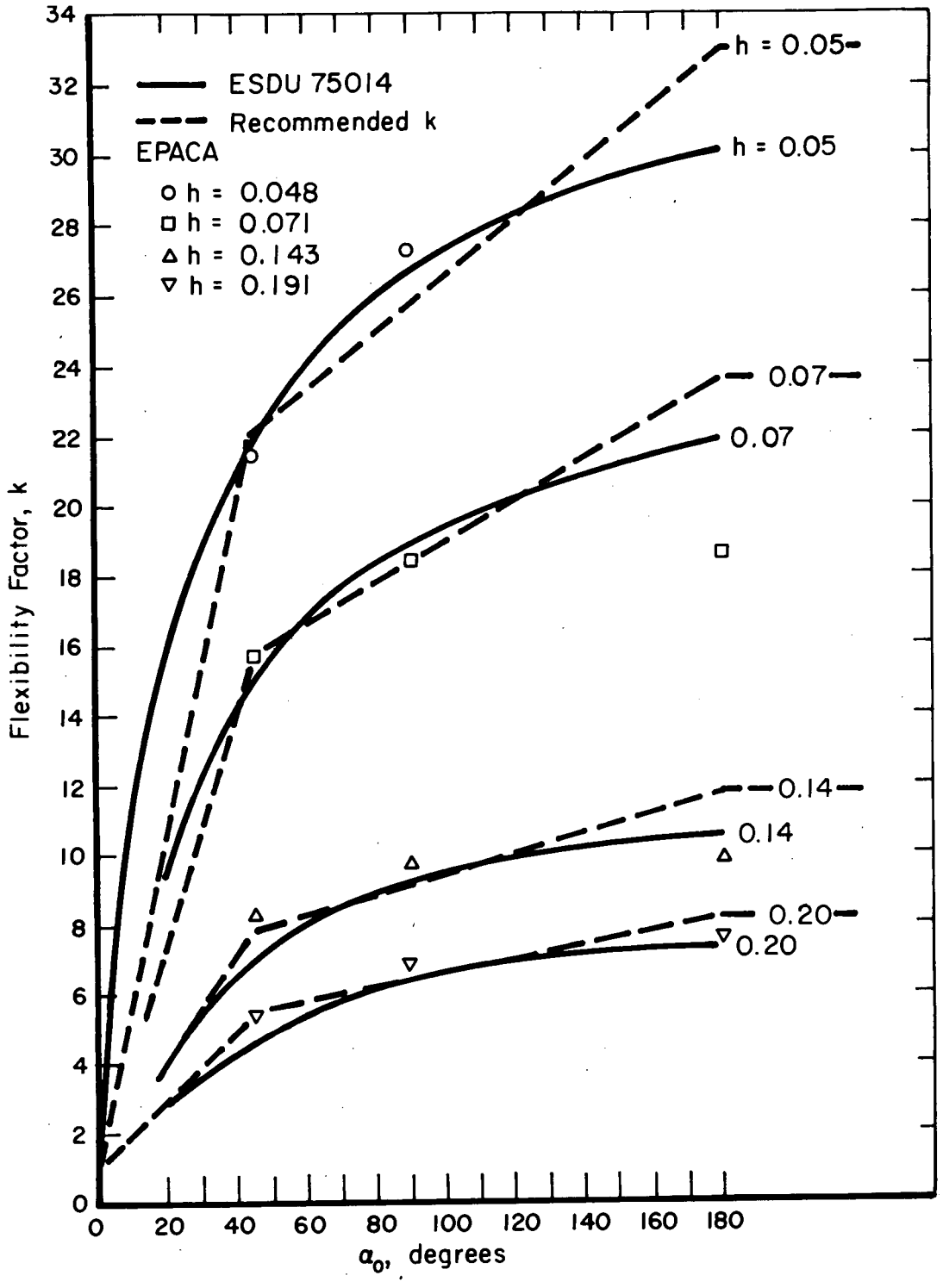

FIGURE 18: COMPARISONS OF FLEXIBILITY FACTORS, IN-PLANE BENDING OF ELBOWS WITH PIPE TANGENTS

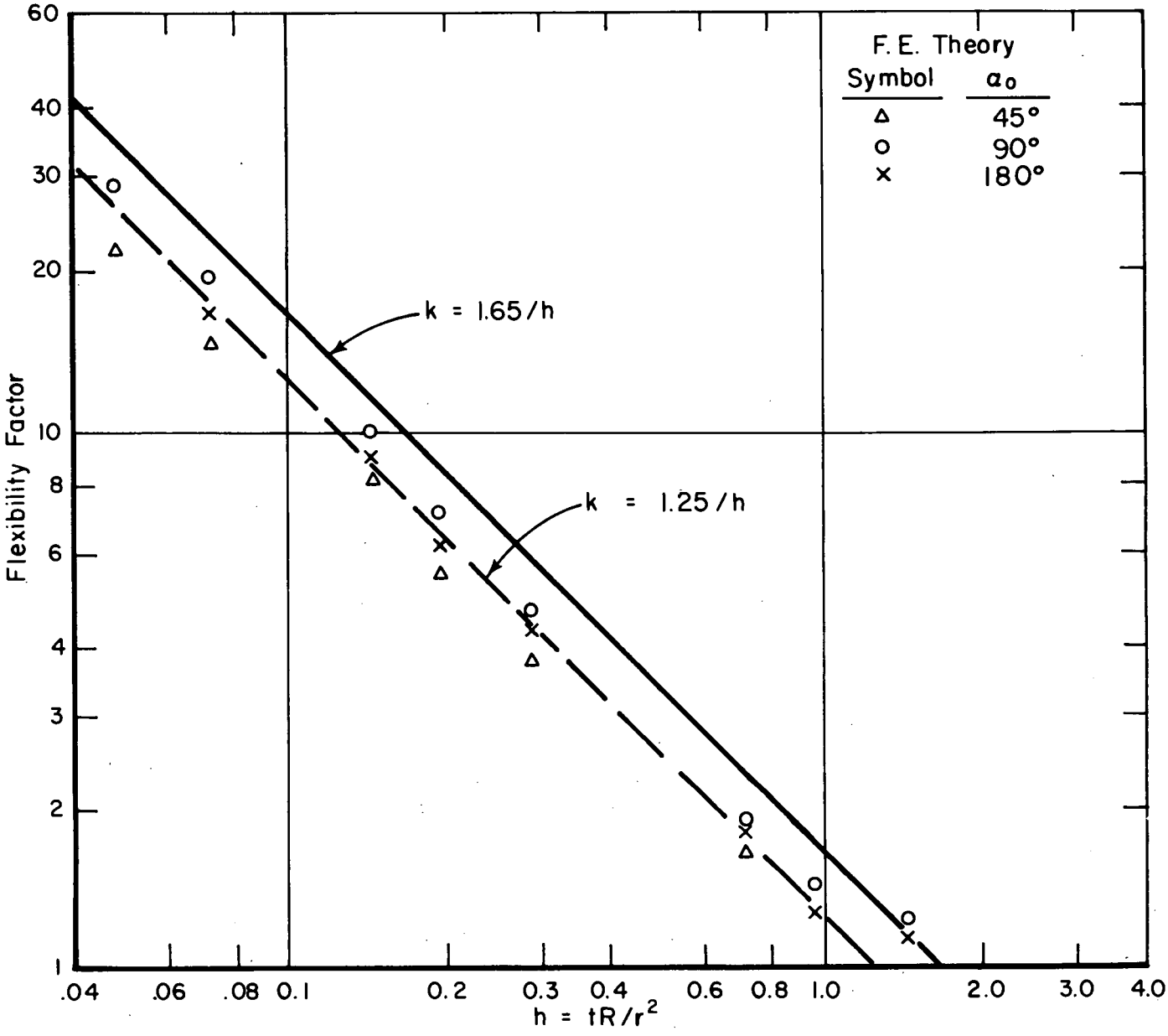

FIGURE 19. OUT-OF-PLANE MOMENT, FLEXIBILITY FACTORS AS A FUNCTION OF h, RECOMMENDED FLEXIBILITY FACTOR EQUATION FOR ALL α_o

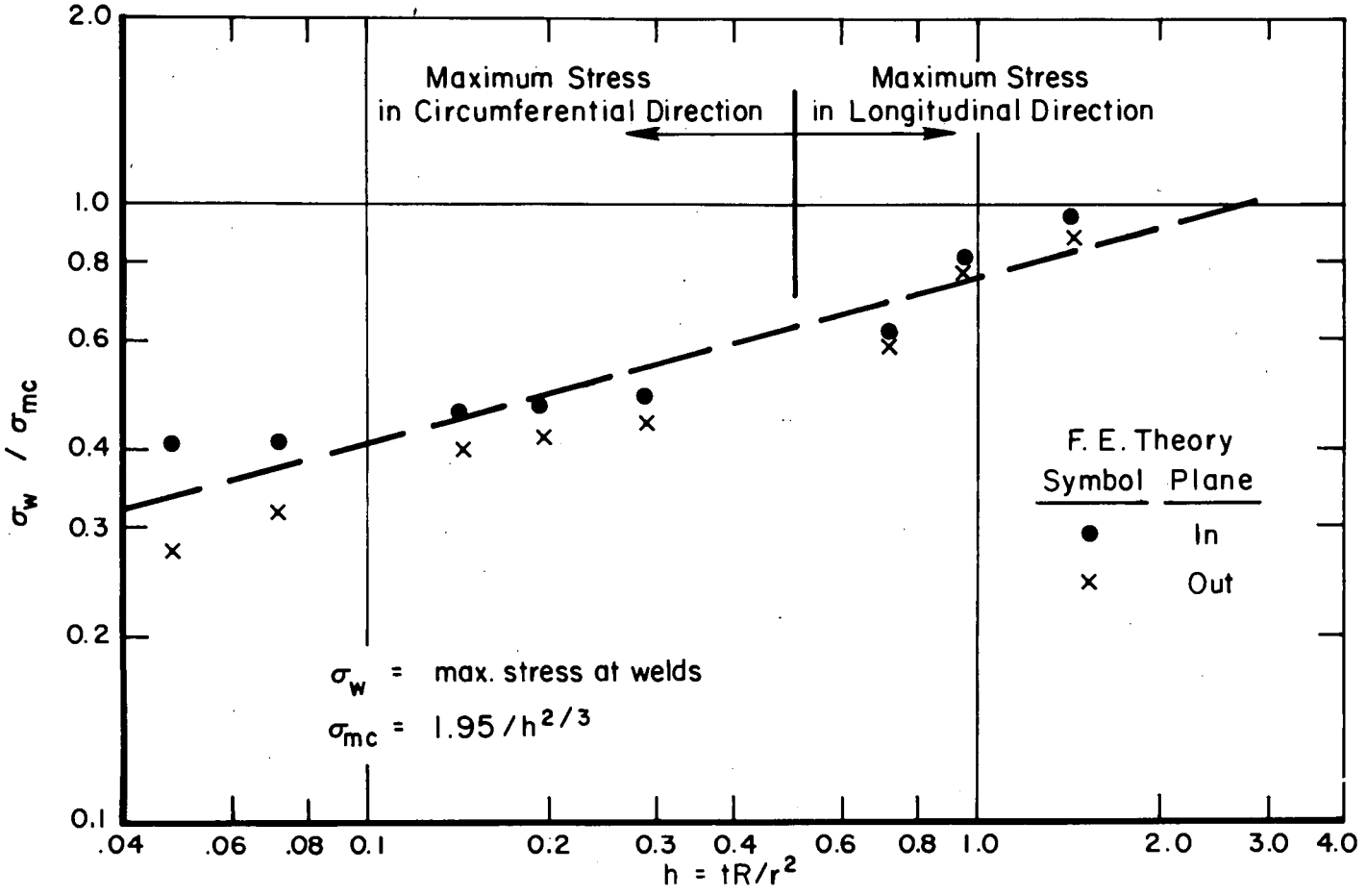

FIGURE 20. MAXIMUM STRESSES AT WELDS (ELBOW-TO-PIPE JUNCTURE)

TABLE 1: DIMENSIONS OF FINITE ELEMENT MODELS

Model No.	λ	R/r	α_o	R, in.	t, in.	L, in.	t_f, in.	r_f, in.	Circ. Elements	Rows of Elements Elbow	Rows of Elements Pipes
1	.05	2	45	20	.238	40.	2.50	15.25	36	5	8
2			90							9	
3			180							12	
4	.075	3	45	30	.238	40.	2.50	15.25	36	5	8
5			90							9	
6			180							12	
7	.15	3	45	30	.477	48.	3.50	16.00	24	5	8
8			90							9	
9			180							12	
10	.20	2	45	20	.954	48.	4.25	17.00	24	3	6
11			90							5	
12			180							10	
13	.30	3	45	30	.954	48.	4.25	17.00	24	3	6
14			90							5	
15			180							10	
16	.75	3	45	30	2.385	50.	7.00	19.50	20	3	5
17			90							5	
18			180							10	
19	1.00	2	45	20	4.770	50.	7.00	19.50	20	3	5
20			90							5	
21			180							10	
22	1.50	3	45	30	4.770	50.	7.00	19.50	20	3	5
23			90							5	
24			180							10	

TABLE 2: IN-PLANE BENDING, SUMMARY OF MAXIMUM CALCULATED STRESSES AND THEIR DIRECTION, SURFACE AND LOCATION

Model No.	λ	$\frac{R}{r}$	α_o, degrees	σ_m/S_n (1)	Dir. (2)	Surface (3)	Location(4) ϕ	Location(4) α
1	.05	2	45	-8.15	C	In	-5	22.5
2			90	-12.91	C	In	-5	45.0
3			180					
4	.075	3	45	-6.97	C	In	-5	22.5
5			90	-10.25	C	In	-5	35.0
6			180	-10.50	C	In	-5	82.5
7	.15	3	45	-4.96	C	In	-7.5	22.5
8			90	-6.60	C	In	-7.5	45.0
9			180	-6.41	C	In	-7.5	97.5
10	.20	2	45	-3.58	C	In	-7.5	22.5
11			90	-5.31	C	In	-7.5	45.0
12			180	-5.96	C	In	-7.5	81.0
13	.30	3	45	-3.04	C	In	-7.5	22.5
14			90	-4.15	C	In	-7.5	45.0
15			180	-4.28	C	In	-7.5	99.0
16	.75	3	45	-2.19	L	Out	-81	22.5
17			90	-2.15	C	In	-9	45.0
18			180	-2.26	C	In	-9	81.0
19	1.00	2	45					
20			90	-2.67	L	Out	-81	45.0
21			180	-2.38	L	Out	-81	135.0
22	1.50	3	45					
23			90	-1.93	L	Out	-81	45.0
24			180	-1.88	L	Out	-81	153.0

(1) σ_m = maximum calculated stress, S_n = nominal stress = $M/\pi r^2 t$

(2) C = circumferential, L = longitudinal

(3) In = inside surface, Out = outside surface

(4) See Figure 1 for definition of coordinate angles ϕ and α

TABLE 3. IN-PLANE BENDING, SUMMARY OF FE-THEORY MAXIMUM INTERPOLATED STRESSES AND COMPARISON WITH NEE-THEORY MAXIMUM STRESSES

Model No. (5)	λ	$\frac{R}{r}$	α_o, degrees	σ_{mi}/S_n (1)	Dir. (2)	Surface (3)	Location(4) ϕ	Location(4) α
1	.05	2	45	8.58	C	In	-5	22.5
2			90	12.93	C	In	-5	45.0
3			180					
Theory			---	15.99	C	In	0	----
4	.075	3	45	7.22	C	In	-5	22.5
5			90	10.31	C	In	-5	35.0
6			180	11.13	C	In	-5	82.5
Theory			---	12.03	C	In	0	----
7	.15	3	45	5.00	C	In	-7.5	22.5
8			90	6.67	C	In	-7.5	45.0
9			180	6.80	C	In	-7.5	97.5
Theory			---	7.62	C	In	0	----
10	.20	2	45	3.64	C	In	-7.5	22.5
11			90	5.31	C	In	-7.5	45.0
12			180	6.10	C	In	-7.5	81.0
Theory			---	6.61	C	In	0	----
13	.30	3	45	3.07	C	In	-7.5	22.5
14			90	4.17	C	In	-7.5	45.0
15			180	4.45	C	In	-7.5	99.0
Theory			---	4.81	C	In	0	----
16	.75	3	45	2.19	L	Out	-81	22.5
17			90	2.16	C	In	-9	45.0
18			180	2.29	C	In	-9	81.0
Theory			---	2.47	C	In	0	----
19	1.00	2	45					
20			90	2.67	L	Out	-81	45.0
21			180	2.39	L	Out	-81	135.0
Theory			---	2.18	C	In	0	----
22	1.50	3	45					
23			90	1.93	L	Out	-81	45.0
24			180	1.89	L	Out	-81	153.0
Theory			---	1.46	C	In	0	----

(1) σ_{mi} = maximum interpolated stress, S_n = nominal stress = $M/\pi r^2 t$

(2) C = circumferential, L = longitudinal

(3) In = inside surface, Out = ouside surface

(4) See Figure 1 for definition of coordinate angles ϕ and α

(5) "Theory" is the NEE (no-end-effects) theory of Ref. (15).

TABLE 4: SUMMARY OF MAXIMUM STRESSES AT WELDS

Model No.	λ	$\frac{R}{r}$	α_o	h	In Plane σ_w/S_n (1)	In Plane σ_w/σ_{mc} (2)	Out-of-Plane σ_w/S_n (1)	Out-of-Plane σ_w/σ_{mc} (2)
1	.05	2	45	.0476	5.46	0.37	4.20	0.28
2			90		6.48	0.44	3.82	0.26
3			180					
4	.075	3	45	.0714	4.51	0.40	3.33	0.29
5			90		4.95	0.44	3.65	0.32
6			180		4.52	0.40	4.12	0.36
7	.15	3	45	.143	3.28	0.46	2.79	0.39
8			90		3.33	0.47	2.75	0.39
9			180		3.13	0.44	2.93	0.41
10	.20	2	45	.191	2.57	0.44	2.33	0.40
11			90		3.01	0.51	2.28	0.39
12			180		2.77	0.47	2.65	0.45
13	.30	3	45	.286	2.11	0.47	1.92	0.43
14			90		2.26	0.50	1.91	0.43
15			180		2.11	0.47	2.02	0.45
16	.75	3	45	.715	1.53	0.63	1.44	0.59
17			90		1.52*	0.62	1.43	0.59
18			180		1.46*	0.60	1.44	0.59
19	1.00	2	45	.954				
20			90		1.69	0.84	1.54	0.76
21			180		1.60	0.79	1.55	0.77
22	1.50	3	45	1.431				
23			90		1.46	0.95	1.35	0.88
24			180		1.46	0.95	1.35	0.88

(1) σ_w = maximum stress at welds. These were obtained from tabulations of the stress along the ϕ-line containing the maximum calculated stress. For in-plane moment σ_w is the average of the 4 elements on each side of the weld, except where marked *; these are averages of the two end elements on the elbow. For out-of-plane moment, σ_w is the average of the 2 elements on each side of the weld at $\alpha = 0$; i.e. the higher-stressed weld zone.

S_n = nominal stress = $M/\pi r^2 t$

(2) σ_{mc} = stress corressponding to Code Stress Index: $C_2 = 1.95/h^{2/3}$.

TABLE 5: OUT-OF-PLANE BENDING, SUMMARY OF MAXIMUM CALCULATED STRESSES AND THEIR DIRECTION, SURFACE AND LOCATION

Model No.	λ	$\frac{R}{r}$	α_o, degrees	σ_m/S_n (1)	Dir. (2)	Surface (3)	Location(4) ϕ	Location(4) α
1	.05	2	45	-6.40	C	In	335	22.5
2			90	7.07	C	In	205	45.0
3			180					
4	.075	3	45	5.23	C	In	205	22.5
5			90	-5.98	C	In	335	35.0
6			180	6.58	C	In	205	22.5
7	.15	3	45	-4.09	C	In	322.5	22.5
8			90	4.09	C	In	217.5	25.0
9			180	4.41	C	In	217.5	22.5
10	.20	2	45	-3.31	L	Out	202.5	22.5
11			90	3.38	C	In	217.5	13.5
12			180	-3.82	C	In	322.5	27.0
13	.30	3	45	-2.63	L	Out	202.5	22.5
14			90	-2.81	C	In	322.5	27.0
15			180	-3.02	C	In	322.5	27.0
16	.75	3	45	-1.83	L	Out	207	22.5
17			90	1.82	L	Out	333	27.0
18			180	-1.85	L	Out	207	27.0
19	1.00	2	45					
20			90	1.86	L	Out	333	27.0
21			180	-1.90	L	Out	207	27.0
22	1.50	3	45					
23			90	-1.54	L	Out	207	27.0
24			180	1.55	L	Out	333	27.0

(1) σ_m = maximum calculated stress, S_n = nominal stress = $M/\pi r^2 t$

(2) C = circumferential, L = longitudinal

(3) In = inside surface, Out = outside surface

(4) See Figure 1 for definition of coordinate angles ϕ and α.

TABLE 6: OUT-OF-PLANE BENDING, SUMMARY OF FE-THEORY MAXIMUM INTERPOLATED STRESSES AND COMPARISON WITH NEE-THEORY MAXIMUM STRESSES

Model No. (5)	λ	$\frac{R}{r}$	α_o	σ_{mi}/S_n (1)	Dir. (2)	Surface (3)	Location (4) ϕ	Location (4) α
1	.05	2	45	6.61	C	In	335	22.5
2			90	7.44	C	In	205	45.0
3			180					
Theory				12.69	C	In	340/200	0.0
4	.075	3	45	5.54	C	In	205	22.5
5			90	6.09	C	In	335	35.0
6			180	6.75	C	In	205	22.5
Theory				9.74	C	In	340/220	0.0
7	.15	3	45	4.11	C	In	322.5	22.5
8			90	4.16	C	In	217.5	25.0
9			180	4.49	C	In	217.5	22.5
Theory				6.18	C	In	335/205	0.0
10	.20	2	45	3.39	L	Out	202.5	22.5
11			90	3.48	C	In	217.5	13.5
12			180	3.91	C	In	322.5	27.0
Theory				5.27	C	In	335/205	0.0
13	.30	3	45	2.70	L	Out	202.5	22.5
14			90	2.87	C	In	322.5	27.0
15			180	3.08	C	In	322.5	27.0
Theory				3.95	C	In	330/210	0.0
16	.75	3	45	1.89	L	Out	207	22.5
17			90	1.92	L	Out	333	27.0
18			180	1.95	L	Out	207	27.0
Theory				2.15	C	In	320/220	0.0
19	1.00	2	45					
20			90	1.94	L	Out	333	27.0
21			180	1.98	L	Out	333	27.0
Theory				1.82	C	In	320/220	0.0
22	1.50	3	45					
23			90	1.62	L	Out	207	27.0
24			180	1.62	L	Out	333	27.0
Theory				1.31	L	Out	165	0.0

(1) σ_{mi} = maximum interpolated stress, S_n = nominal stress = $M/\pi r^2 t$

(2) C = circumferential, L = longitudinal

(3) In = inside surface, Out = outside surface

(4) See Figure 1 for definition of coordinate angles ϕ and α

(5) "Theory" is the NEE (no-end-effects) theory of Ref. (15)

TABLE 7: IN-PLANE MOMENT, SUMMARY OF FE DISPLACEMENTS[1] AND DERIVED FLEXIBILITY FACTORS

Model No.[2]	λ	$\frac{R}{r}$	α_o	δ_x	k_x	δ_y	k_y	θ_z	k_z
1	.05	2	45	-.05226	21.17	-.04477	22.56	.001387	21.40
2			90	-.02659	27.93	-.1683	27.14	.003125	27.30
3			180						
Theory			---	-------	34.63	-------	34.63	--------	34.63
4	.075	3	45	-.05838	14.43	-.04865	15.93	.001425	14.75
5			90	-.03746	17.98	-.1890	18.22	.003153	18.37
6			180	.3698	18.80	-.1791	18.15	.006114	18.61
Theory			---	-------	23.14	-------	23.14	--------	23.14
7	.15	3	45	-.04666	8.15	-.0376	8.81	.0009674	8.24
8			90	-.02562	9.92	-.1245	9.65	.001839	9.67
9			180	.2276	9.87	-.1018	9.78	.003402	9.81
Theory			---	-------	11.55	-------	11.55	--------	11.55
10	.20	2	45	-.02843	5.68	-.02194	5.83	.0006096	5.53
11			90	-.01297	7.79	-.06327	6.94	.001045	6.92
12			180	.1122	7.58	-.03835	7.63	.001908	7.58
Theory			---	-------	8.68	-------	8.68	--------	8.68
13	.30	3	45	-.03099	3.87	-.02336	4.09	.0006186	3.80
14			90	-.01710	4.94	-.06917	4.59	.001039	4.58
15			180	.1201	4.96	-.05629	4.95	.001867	4.92
Theory			---	-------	5.73	-------	5.73	--------	5.73
16	.75	3	45	-.02554	1.82	-.01807	1.80	.0004616	1.63
17			90	-.01323	2.37	-.04289	1.93	.0006308	1.89
18			180	.05910	2.03	-.02956	2.08	.0009703	2.03
Theory			---	-------	2.17	-------	2.17	--------	2.17
19	1.00	2	45						
20			90	-.009452	2.56	-.02984	1.60	.0004881	1.48
21			180	.03526	1.68	-.01413	1.78	.0006830	1.67
Theory			---	--------	1.69	-------	1.69	--------	1.69
22	1.50	3	45						
23			90	-.01214	1.74	-.03521	1.29	.0005219	1.20
24			180	.04164	1.30	.02278	1.36	.0007357	1.28
Theory			---	--------	1.32	-------	1.32	--------	1.32

(1) Displacements are for $S_n = M/\pi r^2 t = 1{,}000$ psi. $E = 3 \times 10^7$ psi

(2) "Theory", in this column, is the NEE-theory.

TABLE 8: IN-PLANE MOMENT, EQUATIONS FOR CALCULATING FLEXIBILITY FACTORS USING FE-THEORY CALCULATED END DISPLACEMENTS

α_o	Equations for Flexibility Factors
45	$k_x = [-\delta_x/(M/EI) - 1.561L^2 - 0.707RL]/[R(0.555L + 0.293R)]$
	$k_y = [-\delta_y/(M/EI) - 1.061L^2 - 0.293RL]/[R(0.555L + 0.0783R)]$
	$k_z = [\theta_z/(M/EI) - 2L]/(0.7854R)$
90	$k_x = [-\delta_x/(M/EI) - 0.5L^2 - RL]/(0.571R^2)$
	$k_y = [-\delta_y/(M/EI) - 1.5L^2 - RL]/[R(1.571L + R)]$
	$k_z = [\theta_z/(M/EI) - 2L]/(1.571R)$
180	$k_x = [\delta_x/(M/EI) - L^2]/[R(3.1416L + 2R)]$
	$k_y = [-\delta_x/(M/EI) - 2RL]/(3.1416R^2)$
	$k_z = [\theta_z/(M/EI) - 2L]/(3.1416R)$

TABLE 9: OUT-OF-PLANE MOMENT, SUMMARY OF FE DISPLACEMENTS(1) AND DERIVED FLEXIBILITY FACTORS

Model No.(2)	λ	$\frac{R}{r}$	α_o	θ_x x 10^4	k_x	θ_y x 10^3	k_y	δ_z x 10^1	k_z
1	.05	2	45	10.90	21.58	0.6283	20.92	0.6005	20.98
2			90	10.48	32.74	1.679	24.91	0.9545	26.92
3			180				-----		
Theory			---	------	34.63	------	34.63	------	34.63
4	.075	3	45	11.20	14.91	0.6581	14.59	0.6701	14.55
5			90	9.950	21.20	1.800	17.71	1.132	18.88
6			180	-30.75	16.58	0.0458	-----	1.372	17.18
Theory			---	-------	23.14	------	23.14	------	23.14
7	.15	3	45	7.393	8.28	0.5219	8.12	0.5493	7.95
8			90	4.837	10.97	1.182	9.06	0.8178	9.60
9			180	-19.17	8.87	0.0021	-----	0.9991	9.00
Theory			---	-------	11.55	------	11.55	------	11.55
10	.20	2	45	4.494	5.46	0.3833	5.35	0.3430	5.12
11			90	2.222	7.97	0.7590	6.17	0.4627	6.55
12			180	-11.03	6.18	0.0001	-----	0.5419	6.32
Theory			---	-------	8.68	------	8.68	------	8.68
13	.30	3	45	4.544	3.77	0.3999	3.73	0.3749	3.55
14			90	1.888	5.08	0.8065	4.28	0.5428	4.53
15			180	-12.02	4.32	<.0001	----	0.6303	4.33
Theory			---	-------	5.73	------	5.73	------	5.73
16	.75	3	45	3.265	1.60	0.3537	1.68	0.3196	1.44
17			90	0.3388	1.98	0.6302	1.84	0.4336	1.91
18			180	-8.203	1.80	<.0001	----	0.4550	1.72
Theory			---	-------	2.17	------	2.17	------	2.17
19	1.00	2	45						
20			90	0.09893	1.60	0.5199	1.31	0.3222	1.50
21			180	-6.043	1.29	0.0001	----	0.2920	1.22
Theory			---	--------	1.69	------	1.69	------	1.69
22	1.50	3	45						
23			90	-0.01371	1.33	0.5742	1.13	0.3947	1.26
24			180	-7.154	1.13	0.0001	----	0.3970	1.07
Theory			---	--------	1.32	------	1.32	------	1.32

(1) Displacements are for $S_n = M/\pi r^2 t = 1{,}000$ psi. $E = 3 \times 10^7$.

(2) "Theory", in this column, is the NEE-theory.

TABLE 10: OUT-OF-PLANE MOMENT, EQUATIONS FOR CALCULATING FLEXIBILITY FACTORS USING FE-THEORY CALCULATED END DISPLACEMENTS

α_o	Equations for Flexibility Factors
45	$k_x = [\theta_x/(M/EI) - 1.4142L + 0.0986R]/(0.6312R)$
	$k_y = [\theta_y/(M/EI) - 1.6263L - 0.3610R]/(0.2777R)$
	$k_z = [\delta_z/(M/EI) - 2.004L^2 - 0.9548RL - .0558R^2]/[R(0.6427L + .25R)]$
90	$k_x = [\theta_x/(M/EI) + 0.65R]/(0.5R)$
	$k_y = [\theta_y/(M/EI) - 2.3L - 1.021R]/(0.7854R)$
	$k_z = [\delta_z/(M/EI) - 1.8L^2 - 2.321RL - 0.65R^2]/[R(0.7854L + 0.5R)]$
180	$k_x = [-\theta_x/(M/EI) -2L - 2.042R]/(1.571R)$
	k_y = not defined
	$k_z = [\delta_z/(M/EI) - 2.042RL - L^2 - 2.6R^2]/(1.571RL)$

TABLE 11: COMPARISONS OF FLEXIBILITY FACTORS FOR OUT-OF-PLANE MOMENTS, ELBOWS WITH $\alpha_o = 90^o$

Model No.	λ	h	$\frac{R}{r}$	k_o (1)	k_t (1)	Assumed(2) k_t=1.0 k_x	k_y
2	.05	.0477	2	31.02	-.422	32.74	24.91
5	.075	.0715	3	20.25	.357	21.20	17.71
8	.15	.143	3	10.50	.826	10.97	9.06
11	.20	.191	2	7.61	.944	7.97	6.17
14	.30	.286	3	4.88	1.104	5.08	4.28
17	.75	.715	3	1.94	1.267	1.98	1.84
20	1.00	.954	2	1.54	1.244	1.60	1.31
23	1.50	1.431	3	1.24	1.265	1.33	1.13

(1) k_o and k_t obtained by simultaneous solution of Equations (4a) and (4b).

(2) k_x and k_y obtained using equations shown in Table 8; these involve the assumption that $k_t = 1$ and that EI/GJ = 1.3.

TABLE 12: EVALUATION OF SIGNIFICANCE OF OUT-OF-ROUNDNESS USING CALCULATED RESULTS FROM REFERENCE (20)

Bending Plane	h	t/r (1)	$\frac{D_{max}-D_{min}}{D}$ (2)	Maximum Stress Ratio for $(D_{max}-D_{min})/D=.025$ (3)	Flexibility Factor Ratio for $(D_{max}-D_{min})/D=.025$ (4)
In	.05	.02	.04	1.02	1.04
	.10	.04	.08	1.03	1.04
	.20	.08	.16	1.03	1.04
	.30	.12	.24	1.04	1.04
	.40	.16	.32	1.04	1.05
	.50	.20	.40	1.03	1.05
Out	.05	.02	.04	0.97	1.05
	.10	.04	.08	0.98	1.03
	.20	.08	.16	0.99	1.03
	.30	.12	.24	0.99	1.04
	.40	.16	.32	0.99	1.02
	.50	.20	.40	0.99	1.03

(1) $t/r = h/(R/r)$, when R/r is assumed to be 2.5

(2) $(D_{max}-D_{min})/D = (\delta_o/t)(t/r)(2)$, with $\delta_o/t = 1.0$

(3) Ratios of stress in elbows with $(D_{max}-D_{min})/D = 0.025$ to stress in circular cross section elbow

(4) Ratios of flexibility factor of elbow with $(D_{max}-D_{min})/D = 0.025$ to flexibility factor of circular cross section elbow